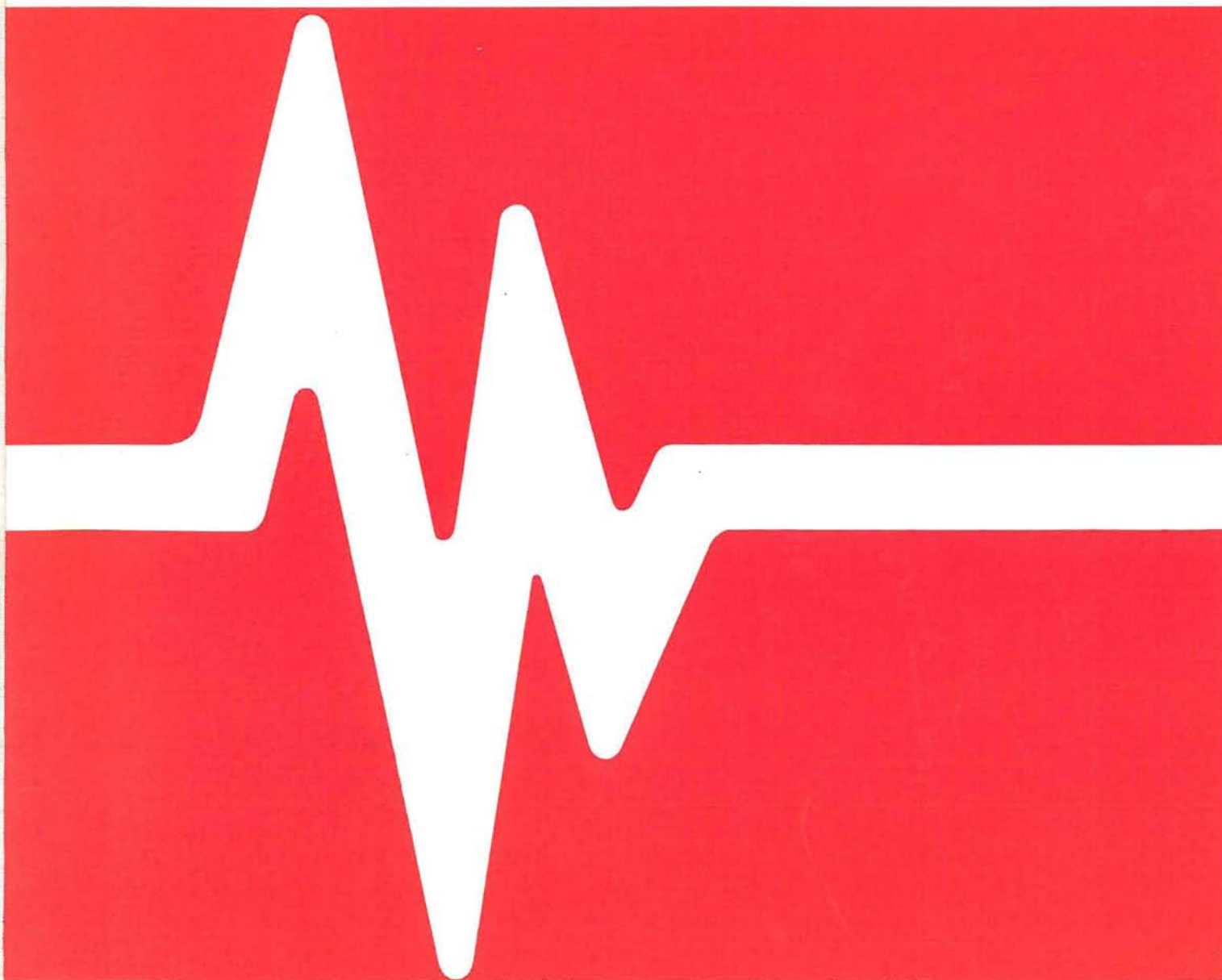


Underwater Noise Exposure
from Shipping in Baffin Bay
and Davis Strait

Ødegaard & Danneskiold-Samsøe K/S



Ødegaard & Danneskiold-Samsøe K/S

Rådgivende ingeniører - Støj og vibrationer
Consulting Engineers - Noise and Vibration

Kroghsgade 1
DK-2100 Copenhagen Ø
Denmark
Telefon: 01-266011
Telex: 19710 oedan dk



Report 87.184

UNDERWATER NOISE EXPOSURE FROM SHIPPING
IN BAFFIN BAY AND DAVIS STRAIT

by

Lars Thiele,
Allan Larsen,
and
Ole Winther Nielsen

for

Greenland Environment Research Institute
Tagensvej 135, 1.
2200 København N

May 1990



<u>CONTENT</u>	<u>PAGE</u>
SUMMARY	3
1. INTRODUCTION	6
1.1 The Effect of Shipping on the Marine Environment ...	7
1.2 Noise Exposure Criteria for Marine Mammals	7
1.3 Underwater Noise Modelling	8
2. NOISE SOURCE LEVELS	10
2.1 Prediction Models	13
2.2 Measured Source Levels Compared with Prediction Models	17
3. SOUND TRANSMISSION LOSS	33
3.1 Sound Propagation in a homogeneous Sea	33
3.2 Sound Propagation in Arctic Waters	35
3.3 Prediction Models	38
3.4 Transmission Loss Measurements	42
3.5 Suggested Transmission Loss Models for Noise Exposure Modelling	44
4. AMBIENT NOISE IN THE SEA	47
4.1 Sources of Ambient Noise in Arctic Waters	47
4.2 Measurements of Ambient Noise in Arctic Waters	49
4.3 Suggested Ambient Noise Spectra for Noise Exposure Modelling	59
5. NOISE EXPOSURE MODEL	62
5.1 General Programme Description	63
5.2 Input Parameters	65
5.3 Output Data	69
6. EXAMPLES OF UNDERWATER NOISE EXPOSURE FROM SHIPPING	72
6.1 Input Data	72
6.2 Results	78
6.3 Discussion	88
REFERENCES	90



SUMMARY

The present report summarizes the work carried out by Ødegaard & Danneskiold-Samsøe ApS in connection with the evaluation of the impact of underwater noise on marine mammals due to shipping activities in the Arctic. The work was initiated in 1980 in connection with the "Arctic Pilot Project" (APP) which was a plan to transport liquefied natural gas (LNG) in large icebreaking tankers year round through Arctic waters. The APP later was abandoned. However, oil and gas exploration still goes on in the Arctic and may result in future projects to ship oil and gas from the Arctic.

The report describes the assessment of underwater noise source strength of icebreaking ships and the ambient noise and transmission loss in Arctic waters. Based on these parameters, a noise exposure computer model has been developed. The actual impact on the marine mammals caused by the underwater noise exposure is not within the scope of this report.

The underwater noise source strength for icebreaking ships is evaluated by comparing field measurements with existing prediction models. The results of the measurements performed by Ødegaard & Danneskiold-Samsøe ApS on the icebreakers "Voima" and "John A. MacDonald" and on the container ship "Jutlandia" are summarized and compared with two prediction models for propeller cavitation noise. This comparison shows that it is possible to predict the underwater noise source strength with a reasonable accuracy. However, at low frequencies a modification is suggested in order to compensate for the high source levels experienced for icebreaking ships in this frequency range.

The factors affecting the sound transmission loss in Arctic waters are described in general and the commonly used prediction models presented. However, it is difficult to predict the sound transmission loss with a satisfactory accuracy due to the complex nature of sound propagation. If detailed results are required for a certain area and for certain conditions, measurements will be



necessary. The results obtained from measurements performed by Ødegaard & Danneskiold-Samsøe ApS at Baffin Bay and Lancaster Sound are presented and compared with predicted losses using a computer model.

The sound transmission loss to be used as input for the underwater noise exposure programme preferably should be data values derived either from measurements or from separate calculations using a detailed prediction model. However, to use the exposure programme when no such detailed transmission loss data are available, a simple transmission loss prediction model is presented and included in the exposure programme.

The special aspects of the ambient underwater noise in Arctic areas are commented in general. The results of measurements carried out by Ødegaard & Danneskiold-Samsøe ApS are presented and compared with other investigations. It is noted that the noise level is strongly influenced by the presence of the ice and very dependent on the weather and temperature conditions.

Based on the measured data, suggestions are given for a set of spectra of typical average ambient noise in a summer and a winter condition. The magnitude of the selected average ambient noise levels is lower during winter than during summer conditions.

When the source strength, transmission loss and ambient noise are combined, the noise exposure at a certain receiver can be evaluated. The noise exposure model described in this report is based on a criteria defined as exposure occurs when the time averaged ship noise level is higher than the average ambient noise. In order to evaluate the impact due to a certain shipping activity, it is important to know the area and period of time where the noise exposure occurs.



The present underwater noise exposure model has been developed with the aim of presenting visualized and easy interpretative results which illustrate the extent and duration of noise exposure due to shipping. The input for the computer programme is a ship route with sailing conditions, various source strengths along the route, the sound transmission loss in the area, and the ambient noise level. The output from the programme is an exposure map which fits together with a sea chart showing contour lines of the time averaged noise level above ambient noise and a "waterfall" display illustrating the variation with time of the received or detected noise spectra at an observation point.

Five examples have been calculated in order to illustrate the use of the underwater noise exposure programme. The ships used for the examples are the icebreaker "John A. MacDonald", the planned LNG-carrier from the APP project and a small ship at the size of a fishing trawler or seismic ship. The routes applied are one route through central Baffin Bay and two routes along the west coast of Greenland.



1. INTRODUCTION

The past decade has seen an increased interest in exploring oil and gas resources in the Arctic. Proposals have been put forward for the development of production fields in the Arctic as well as transportation systems made up of ships or pipelines to deliver hydrocarbons in large quantities from the Arctic to markets in Canada/U.S.A. or Europe.

One of these projects, the "Arctic Pilot Project" (APP), presented in the late 1970-ies by a Canadian consortium, planned to ship liquified natural gas (LNG) in large ice-breaking tankers, capable of operating all year round. The LNG-carriers were to navigate a route between the loading terminal situated in eastern Arctic Canada and unloading terminals located on the Canadian east coast or in Europe. On this route the LNG-carriers were to pass through the Baffin Bay and Davis Strait, waters which presently are not encountered by regular ship traffic and only rarely used for winter navigation. However, in 1983 the project was abandoned.

As part of an assessment of the environmental impact of the APP, caused by the suggested shipping in Greenland waters, underwater noise from the ships was identified as a possible major environmental hazard. Great efforts were made to describe the extent of the noise impact and several studies were made as described in the following. The purpose of this report is to compile the main information collected during this work and to present the assessment of noise exposure caused by the LNG-carriers. This assessment is based on a computer noise exposure model which is presented for the first time in this report. Apart from the assessment of the noise from the APP tankers, the model developed may also be used in estimating the noise exposure caused by other shipping in west Greenland or wherever shipping noise is expected to be a problem.



1.1 The Effect of Shipping on the Marine Environment

The advent of the Arctic Pilot Project and similar projects have resulted in the recognition of a number of problems connected with navigation in Arctic waters.

Concern has thus been expressed at the possible impact the proposed increase in ship traffic may have on the marine environment along future shipping routes. In particular attention has been drawn to the underwater noise generated by the LNG-carriers which will change the acoustic environment of the sea on which the life of marine mammals is vitally dependent.

The proposed ship traffic will generate underwater noise which will propagate in the sea and increase the noise level at a distance from the ships. Increased noise levels may affect the marine mammals living in the area. The noise may in particular interfere with their ability to communicate, navigate and locate their food and hence deteriorate their conditions of life.

1.2 Noise Exposure Criteria for Marine Mammals

Assessment of the impact of underwater noise must be made in accordance with appropriate noise exposure criteria for the various species of marine mammals. Such criteria, stating permissible noise levels and exposure times, are, however, not available at the present but is a topic on which behavioural research efforts are focused. The possible low frequency masking effects that can be ascribed to underwater noise radiated by ships are of major concern in particular to large marine mammals such as baleen whales which are known to use low frequency vocalization for communication. The marine mammals will also be influenced by the masking of the natural sounds which are used by the mammals for orientation and localization of prey, the so-called passive sonar.



The present report will not consider this issue further. The scope of the report is solely to cover a noise exposure model which will show the potential zones and times influenced by the underwater noise and hence the potential for disturbance of marine mammals. The extent to which different marine mammal species might be disturbed will not be considered.

1.3 Underwater Noise Modelling

The basis needed for predicting underwater noise exposure is furnished by the passive sonar equation as for instance given by Urick /1/. The equation includes the parameters of interest to the problem at hand and describes how they interact to yield the sound level to be detected above the ambient noise by an omnidirectional receiver at a distance from a given source of underwater noise. The choice of omnidirectional receiver characteristics rests with the fact that very little is known about the sound perception of the animals in question.

For the present purpose the passive sonar equation reads:

$$L_d = L_s - TL - L_a \quad (1)$$

where

- L_d is the detection level above ambient
- L_s is the source strength level
- TL is the transmission loss and
- L_a is the ambient noise level

All quantities are to be measured in dB and are in general functions of frequency and time.

Knowledge and understanding of the parameters appearing on the right hand side of equation (1), combined with the knowledge of the particulars of ship design and sailing conditions on a specific route, make it possible to predict the noise level to be detected above ambient noise and hence estimate the noise exposure at a certain geographical location.

The source strength L_s of a ship is a frequency dependent measure of the sound level radiated to the surrounding body of water. The source strength of ships is usually calculated from empirical or deterministic mathematical models which reflect the noise generation processes involved. Determination of the source strength of a given ship usually requires information about principal dimensions, operating and loading conditions.

The transmission loss TL is a frequency dependent measure of the attenuation of sound waves with range. The transmission loss determines the decrease in sound level that can be detected at a distance from the noise source. The transmission loss which is independent of the noise source, may be calculated from empirical or deterministic models which include the topographical and oceanographical characteristics of the region as well as the location of the source and the receiver.

Spectra of the ambient noise level L_a give a frequency dependent measure of the sound levels that occur naturally in a particular region of interest. Ambient noise in the sea originates from a wide variety of noise sources such as biological activity, impact of the sound from raindrops, breaking of waves, release of air bubbles in ice or surface water, cracking of ice or distant shipping routes. The complex nature and possible seasonal changes of ambient noise spectra make reliable theoretical predictions impossible. Hence assessment of ambient noise can only be made by means of measurements in the regions of interest.

Table 1.1 below presents a list of the parameters, reference locations and short definitions given as ratios which are appropriate to the passive sonar equation (1). More complete definitions of the parameters will be given in the following chapters which cover the various parameters in detail.



Parameter/ symbol	Reference location	Definition
Source level L_S	1 m from source centre	$10 \log \frac{\text{Source intensity}}{\text{reference intensity}^*}$
Transmission loss TL		$10 \log \frac{\text{Signal intensity at 1 m}}{\text{signal intensity at receiver}}$
Ambient noise level L_a	at receiver location	$10 \log \frac{\text{Noise intensity}}{\text{reference intensity}^*}$
Detection level L_d	at receiver location	$10 \log \frac{\text{Signal power at receiver}}{\text{noise power at receiver}}$

* The reference intensity is the intensity of a plane wave of 1 μPa rms pressure

Table 1.1.

The sonar parameters, their definitions and reference locations.

2. NOISE SOURCE LEVELS

In general ships must be regarded as composite sources of underwater sound. Rotating and reciprocating machinery, necessary for the operation of the ships, generate vibrations which, when transmitted through the hull structure into the sea, appear as underwater noise. Main engines, auxiliary engines, compressors and gears, which are found to be the main sources of machinery noise, produce a line-component noise spectrum depending on the rate of revolutions of the particular machinery involved.

Of particular importance is the propeller(s) of a ship which is responsible for the conversion of the rotative energy developed by the main engines, into a thrust force suitable for propulsion.

When a propeller operates in water, low pressure regions will form on the blade surfaces and in the core of the vortices trailing the blade tips. If the pressure in these regions falls below the vapour pressure of water, vapour filled pockets known as ca-



itation bubbles will be formed. The cavitation bubbles are not stationary relative to the propeller but are convected by the water flow across the blade surfaces into regions where the pressure exceeds the vapour pressure which causes the cavitation bubbles to collapse. The random formation and collapse of a large number of individual cavitation bubbles constitute a significant source of broad band noise which lend itself to analysis by means of statistical methods.

The spectrum shape typical for broad band propeller cavitation noise is characterized by steep increase in noise level with frequency towards a broad hump, centering around a peak frequency determined by propeller loading and rate of revolutions. At frequencies above the peak frequency, the noise level starts to decrease, slowly at first until it rolls off at a constant rate of -6 dB per octave. Broad band cavitation noise is often found to dominate underwater noise spectra from ships at frequencies above 100 Hz - 200 Hz.

The wake flow in the propeller aperture of a ship is usually found to vary in space due to presence of the hull upstream of the propeller. The blades of a wake operated propeller are thus subjected to periodically varying flow conditions which in turn will cause periodic variations of the gross volume of cavitation bubbles forming on the blades. The cyclic variation of the extent of the cavitating region will produce a line-component noise spectrum at integer harmonics of the blade rate frequency. These spectral lines are known as blade tonals.

Of the three major noise sources just described, noise from cavitating propellers is found to dominate the spectra of radiated underwater noise under most conditions. The relative importance of the three sources described above are, however, dependent on the design of a given ship and in particular of the loading condition under which the ship operates. This is illustrated in Figure 1.1 which shows the characteristics of the spectrum of ship noise at two different loading conditions.

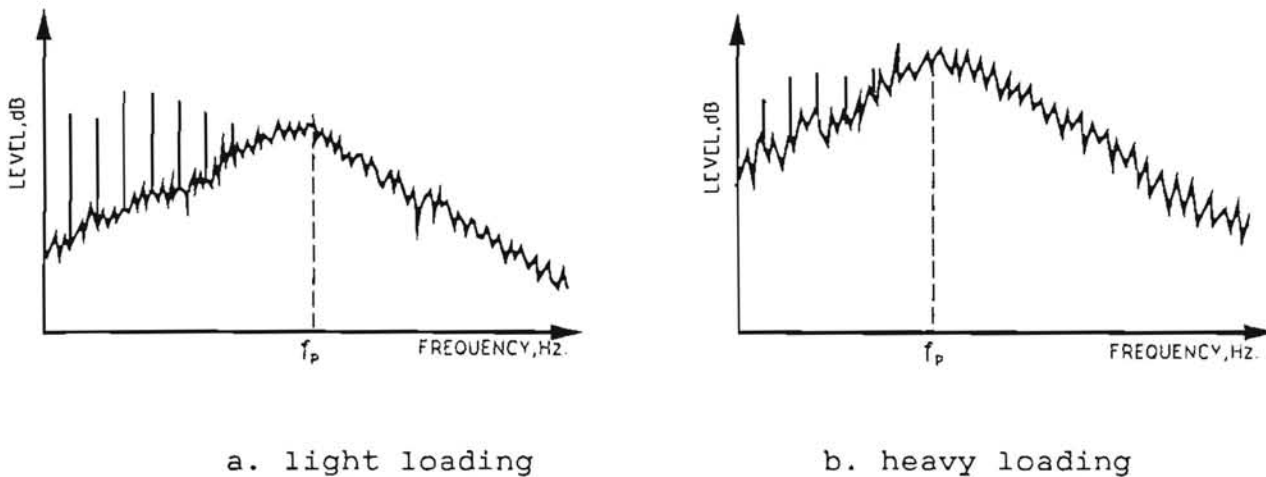


Figure 1.1.
Schematic spectra of radiated underwater noise from a ship at two different loading conditions.

Figure 1.1a shows a schematic spectrum at a light loading condition which results in little propeller cavitation. The low frequency end of the spectrum is dominated by spectral lines due to the machinery, and the blade tonals of the propeller. These lines die away with increasing frequency and vanish in the continuous spectrum of broad band cavitation noise.

At high propeller loadings the level of the broad band noise increases and the peak frequency shifts towards lower frequencies as shown in Figure 1.1b. At the same time some of the line components increase in both level and frequency, but in general the broad band contribution becomes predominant. Underwater noise spectra obtained from icebreaking vessels and fast passenger or cargo ships which operate at high propeller loadings are thus found to be dominated by broad band cavitation noise at frequencies typically above 100 Hz.



2.1 Prediction Models

Prediction of the underwater noise spectrum L_d to be detected above ambient noise at a distance from a particular ship, involves assessment of the source strength L_s of the ship, the transmission loss TL from the source to the receiver and the ambient noise level L_a at the receiver location. Once these quantities are known sufficiently detailed, the noise exposure may be calculated according to equation (1). The present section covers the prediction of the noise source strength L_s , whereas prediction of the transmission loss TL and assessment of the ambient noise level L_a are treated in sections 3 and 4, respectively.

The equivalent noise source strength or source level L_s referred to above is a standard concept used in underwater acoustics which allows noise ratings of ships made at different geographic locations to be compared on equal basis. The source strength of the ship noise is defined as the noise level that would be measured at a distance of one metre from an imaginary monopole source, placed at the acoustic centre of the ship and having an acoustic intensity similar to that of the ship. The equivalent source strength L_s is conveniently referred to the intensity of a plane wave having an rms pressure of 1 uPa and is given as spectrum levels in 1 Hz bands.

A detailed deterministic prediction of the noise source strength spectrum of a ship is quite complicated to perform and requires comprehensive knowledge of the structural and hydrodynamic design parameters of the ship in question. Such information may not always be available to the noise analyst, hence an empirical formulation of the source level spectrum, based on statistical properties of ship noise, appears attractive.

Source Level Model due to Ross

Ross /2/ recognized that propeller cavitation is the dominating noise source for surface ships operating at cruise speed and at



medium to heavy propeller loadings. This observation combined with a large amount of ship noise data obtained from naval sound ranges have led to the suggestion of a simple empirical relation for the source level spectrum L_S , valid for surface ships being more than 100 m long and having propeller tip speeds in the range 15 m/s to 50 m/s. The Ross prediction model for noise source strength reads,

for $f \geq f_p$:

$$L_S = 195 + 60 \log(V_t/25 \text{ m/s}) + 10 \log(B/4) - 20 \log(f) \quad (2)$$

and for $f \leq f_p$:

$$L_S = 195 + 60 \log(V_t/25 \text{ m/s}) + 10 \log(B/4) - 20 \log(f_p)$$

where L_S is the source level in dB re. $1 \mu\text{Pa}/\text{Hz}^{1/2}$
 V_t is the propeller tip speed in m/s
 B is the total number of propeller blades
 f_p is the peak frequency equal to 100 Hz and
 f is the frequency.

The source spectra predicted by (2) are of constant level from low frequencies to the peak frequency f_p at 100 Hz. Above 100 Hz the spectrum rolls off at a rate of -6 dB per octave in accordance with stochastic theories of cavitation noise. Reference is made to a paper by Baiter et al. /3/.

The source level model given in equation (2) represents an average of a large number of ship noise spectra, hence a measured noise spectrum from a particular ship is expected to show more structure than predicted by equation (2). Ross states that the source level model is expected to deviate from measured spectra by 1 dB to 3 dB in the frequency range above 100 Hz. In the frequency range below 100 Hz the present source level model is known to underpredict measured source levels by 2 dB to 8 dB. This



effect may be attributed to the presence of propeller blade tonals and machinery components in the frequency range below 100 Hz.

The source level model suggested by Ross assumes a fixed peak frequency of 100 Hz and thus fails to recognize the tendency of f_p to decrease with increasing propeller diameter. Ødegaard & Danneskiold-Samsøe has suggested a slight modification of the Ross model according to which the peak frequency is determined by the following relation:

$$f_p = 300 / D \text{ (Hz)} \quad (3)$$

where D is the propeller diameter in metres.

Application of a peak frequency given by equation (3) in the Ross model (2) yields source levels which are in fair agreement with measured source levels as will be illustrated in the Section 2.2.

Source Level Model Due to Brown

The source level model due to Ross fails to predict the shift of peak frequency at high loadings towards lower frequencies as shown in Figure 1.1. Also the source level model fails to recognize the influence of propeller design and loading condition on radiated ship noise. These shortcomings are to some extent remedied by another prediction model suggested by Brown /4/ and /5/. According to Brown the equivalent monopole source level L_S of the propeller of a ship may be predicted from the following empirical relation,

for $f \geq f_p$

$$L_S = K + 40 \log(D) + 30 \log(n) + 10 \log(B) + 10 \log(A_C/A_D) - 20 \log(f)$$

(4)



and for $f \leq f_p$

$$L_S = K + 40 \log(D) + 30 \log(n) + 10 \log(B) + 10 \log(A_C/A_D) - 20 \log(f_p)$$

L_S is the source level in dB re. $1 \mu\text{Pa}/\text{Hz}^{1/2}$

K is 170 dB for a thruster and 163 dB for an open propeller

D is propeller diameter in metres

n is the rate of propeller revolutions rev./sec.

B is the number of blades

A_C is the swept area of cavitation

A_D is $\pi \cdot D^2/4$ i.e. the propeller disk. area and

f is the frequency

f_p is the peak frequency

The peak frequency, or "break" frequency, f_p appearing in equation (4) may according to Brown be determined from the following equation,

$$f_p = \frac{1100}{D} \left(\frac{V_t}{V_i} \right)^{-2/3} \quad (5)$$

$$\text{for } \frac{V_t}{V_i} > 1.5$$

where V_t/V_i is the ratio of actual propeller tip speed to the tip speed at cavitation inception.

The relation between V_t , V_i and f_p given in equation (5) was based on noise measurements and cavitation inception observations in model scale. Field measurements to be discussed in details in the next section, do, however, suggest a modification of equation (5) in order to obtain better accordance between measured and predicted noise source levels. The modified equation reads,



$$f_p = \frac{550}{D} \frac{v_t}{v_i}^{-2/3} \quad (6)$$

which introduces a 6 dB increase of the noise source level below the peak frequency which in turn is shifted towards lower frequencies.

2.2 Measured Source Levels Compared with Prediction Models

The modified prediction models for the equivalent noise source strength L_s of ships, due to Ross and Brown, have been compared with measured source level spectra of two icebreakers and a fast container ship in order to evaluate the ability of the models to predict underwater noise from high powered ships operating in open waters or waters covered with ice. The three cases investigated are covered in separate sections given below.

"M/S VOIMA"

The measurements reported by Thiele /6/ are concerned with underwater noise radiated by a Finnish icebreaker operating under various loading conditions in the Gulf of Bothnia. The 1100 DWT icebreaker M/S VOIMA which is owned and operated by the Finnish Board of Navigation, is of the Baltic type and is powered by a 12800 kW DC-diesel electric propulsion unit. The ship is equipped with two 4 bladed 3.0 m diameter fixed pitch propellers fore and two 4 bladed 4.2 m diameter fixed pitch propellers aft. The profile of M/S VOIMA is shown in Figure 2.1 below.

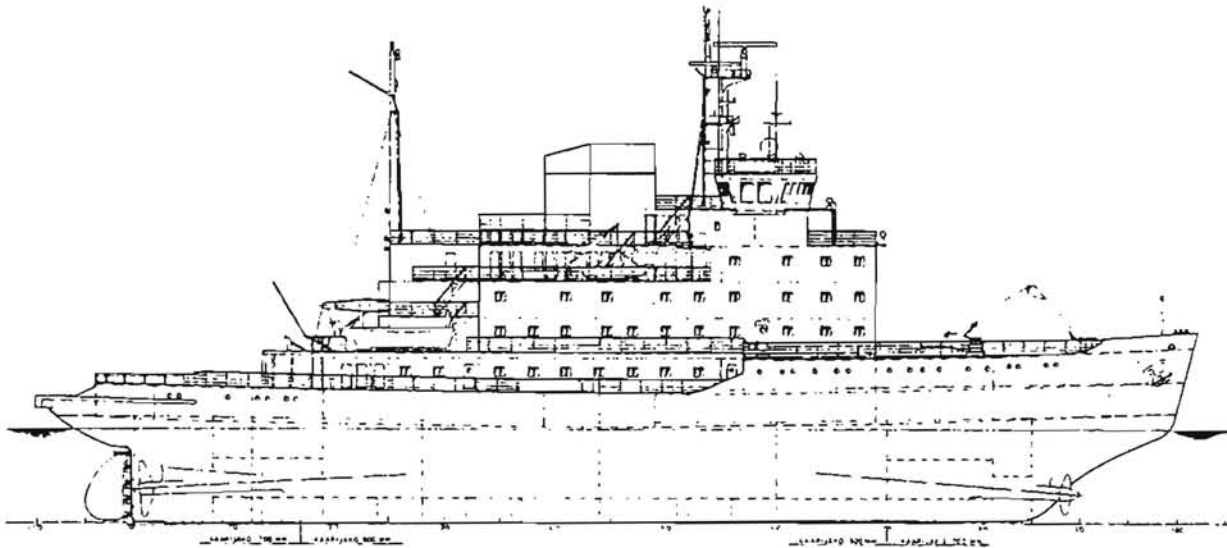


Figure 2.1.
Elevation plan of the icebreaker M/S VOIMA.

The noise measurements were made by means of 3 hydrophones suspended at a depth of 30 m below the ice cover which consisted of 0.3 m thick pack ice. The distance from the icebreaker to the receiver locations was monitored continuously during the noise recordings along with information on engine load, propeller rpm and ship speed. The weather was calm during the tests with air temperatures ranging between 0°C and 5°C.

All recorded noise data were analysed in 1/3-octave bands in the frequency range 25 Hz - 5 kHz and converted to source levels referring to 1 m distance from the icebreaker by correcting the measured noise levels for the appropriate transmission losses. Since no transmission loss measurements were made during these tests, estimated transmission losses according to a method due to Marsh and Schulkin /7/ was applied during the data reduction procedure. The estimated transmission losses corresponded to attenuation by spherical spreading corrected for an empirically determined frequency dependent near-field anomaly.



Figure 2.2 compares the source level spectrum L_s measured during icebreaking with the source level spectrum predicted by the model due to Ross but modified according to equation (3). During the measurements the M/S VOIMA was propelled by the aft propellers which were operating at 100% load corresponding to 120 rpm. The bow propellers were running at the lowest possible rpm and did not have any significant influence on the radiated noise.

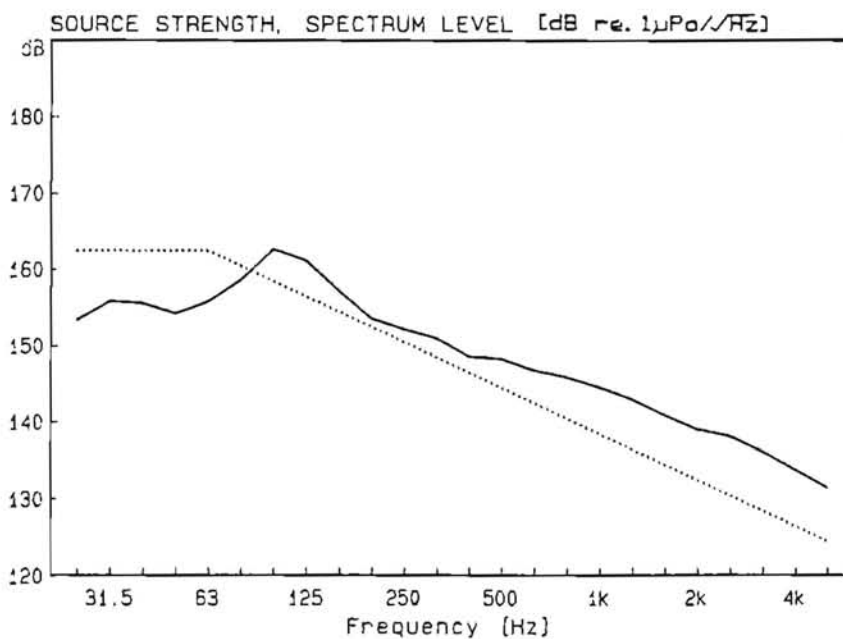


Figure 2.2.
Measured and predicted source level spectra during icebreaking. Aft propeller rpm: 120. Aft propeller load 100%.

Full line : Measured.
Dotted line: Brown.

As seen from Figure 2.2 the predicted source level spectrum agrees fairly well with the measured values although certain discrepancies are apparent at high and low frequencies. The discrepancy at low frequencies may be attributed to an under prediction of the transmission loss by the Marsh and Shulkin model whereas the excess at high frequencies is believed to indicate that icebreakers are more noisy than the bulk of the ships which



form the statistical background for the Ross model. This assumption is supported by Figure 2.3 which compare the overall noise source levels above 100 Hz, L'_S , obtained from M/S VOIMA with the same data for a group of ships analysed by Ross /2/.

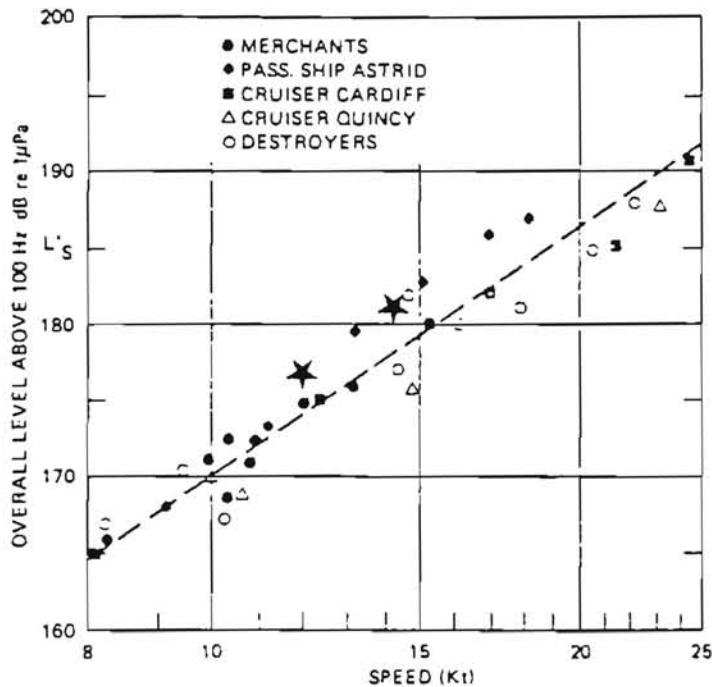


Figure 2.3.

A comparison between measured overall noise levels L'_S from M/S VOIMA (★) and overall noise levels from a group of ships. Figure adopted from Ross /2/.

"M/S JUTLANDIA"

Measurements of underwater noise from a large triple screw container ship made in the Skagerrak have been reported by Thiele /8/. The 274 m long container ship M/S JUTLANDIA which is owned and operated by EAC, is powered by a 55,000 kW two-stroke diesel propulsion plant connected to a 4 bladed 6.5 m controllable pitch propeller situated in the centre line and two 6 bladed 5.85 m fixed pitch propellers situated in port and starboard side. The profile of M/S JUTLANDIA is shown in Figure 2.4 below.

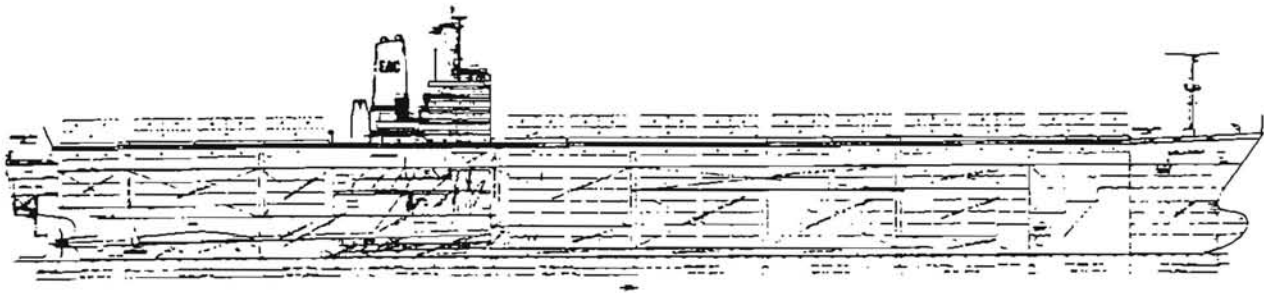


Figure 2.4.
Elevation plan of the container ship M/S JUTLANDIA.

The noise measurements were made by means of a hydrophone suspended from a pilot boat at depths of 50 m and 89 m below the sea surface. The distance from the container ship to the pilot boat was monitored continuously and recorded along with the noise data and information about the engine load and speed of the container ship. The weather was relatively calm during the measurements with north westerly winds of 3-5 m/s and minor waves corresponding to sea state 2.

All recorded noise data were analysed in 1/3-octave bands in the frequency range 25 Hz - 5 kHz and converted to source levels referring to 1 m distance from the ship by correcting the measured noise levels for the appropriate transmission losses measured at four ranges upon completion of the ship noise recordings which covered three different engine/propeller loads as given in Table 2.1 below. The measured source level spectrum presented for each load condition is finally obtained as an average of the individual source level spectra.

Application of the Ross model for prediction of source level spectra is straight forward once the diameter of the propeller and the relevant propeller revolutions for a certain loading to be analysed are known.



Cond. No.	Ship speed (kN)	Centre eng. power (kW)	Centre prop. rpm	Wing. eng. power (kW)	Wing prop. rpm
1	27	22,820	115	16,190 stb. 15,460 pt.	114 113
2	9-19	8,100- 24,140	75-112	0 stb. 0 pt.	Wind milling
3	19	23,180	114	0 stb. 0 pt.	Wind milling

Table 2.1.
Loading conditions of the M/S JUTLANDIA subjected to underwater noise measurements.

Cond. No.	Mode	V_t/V_i	A_c/A_D
1	Constant speed	2.0	0.15
2	Start acceleration	3.8	0.20
2	End acceleration	3.8	0.40
3	Constant speed	3.0	0.30

Table 2.2.
Cavitation parametres estimated for M/S JUTLANDIA.

Application of the prediction model suggested by Brown is not quite as simple as application of the prediction model due to Ross because the cavitation inception speed V_i of the propeller and the swept area of cavitation A_c are not as easy to obtain as the other variables occurring in equations (4) and (6). V_i and A_c are functions of the load condition and the wake flow of a particular ship and accurate assessment of the cavitation inception speed and the swept area of cavitation requires elaborate calculations or model experiments to be performed. Less accurate but useful estimates for V_i and A_c can be obtained by exercising



experience and engineering judgement. The numerical values of V_t/V_i and A_C/A_D applied by Thiele /8/ for loading conditions 1, 2 and 3 are based on estimates performed by N. Brown for M/S JUTLANDIA. The values are given in Table 2.2.

Figures 2.5 - 2.8 below compare the measured source level spectra L_S obtained during the tests with the source level spectra predicted by the modified Ross model, equations (2) and (3), and the modified Brown model, equations (4) and (6).

The predicted source level spectrum for condition 1, which involves noise contributions from 3 propellers, was obtained by adding the source level spectra from the individual propellers on energy basis.

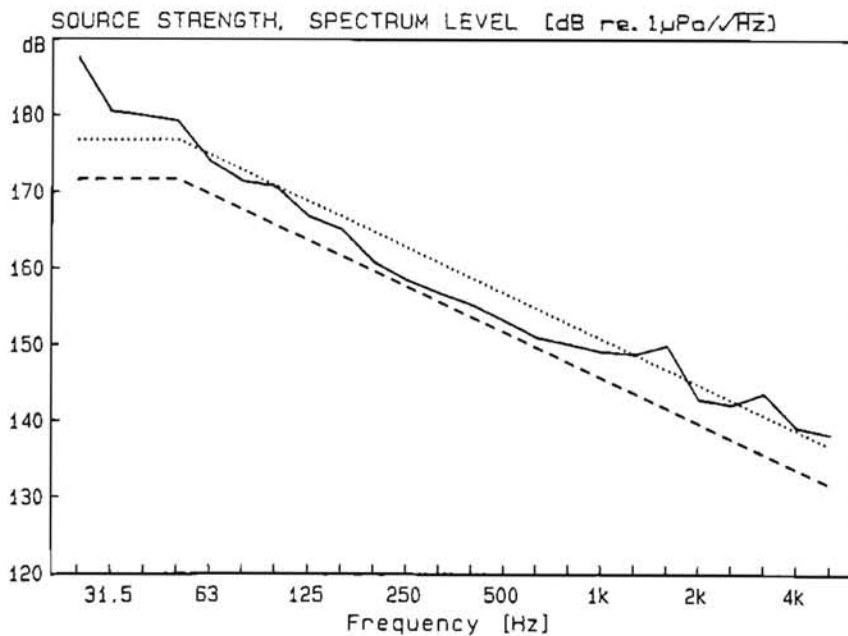


Figure 2.5.
Measured and predicted source level spectra for load condition 1.

Measured: ———, Ross, modified: ······,
Brown, modified: - - - - -

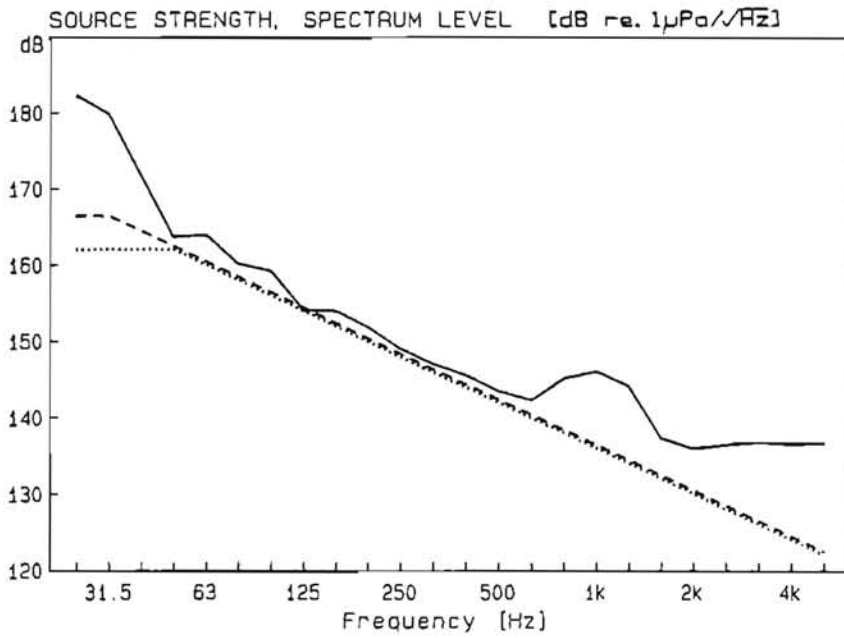


Figure 2.6.
Measured and predicted source level spectra for load condition 2, start of acceleration (75 rpm).

Measured: ———, Ross, modified : ······,
Brown, modified: - - - - -

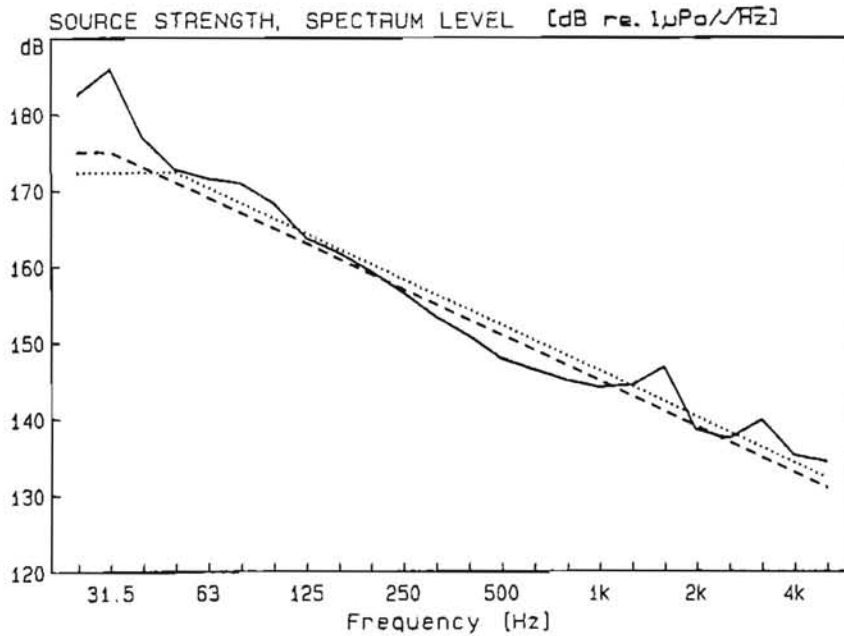


Figure 2.7.
Measured and predicted source level spectra for load condition 2, end of acceleration (114 rpm).

Measured: ———, Ross, modified : ······,
Brown, modified: - - - - -

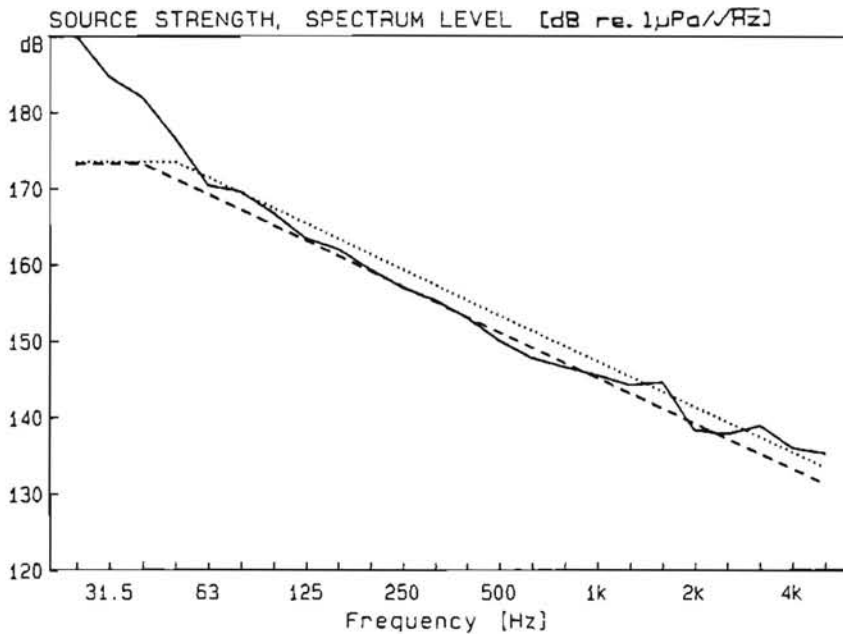


Figure 2.8.
Measured and predicted noise level spectra for load condition 3.

Measured: ——— , Ross, modified: ······,
Brown, modified: - - - - -

As seen from Figures 2.5 - 2.8 the modified source level models due to Ross and Brown predict source strength spectra which are in fair agreement with the measurements at frequencies above 50 Hz. Below 50 Hz the measured source strength spectra exceed the predictions by 8-12 dB, an effect which is due to propeller and engine tonals in the measured noise signal and thus not accounted for by the prediction models. The peaks which are present at 1.6 kHz and 3.15 kHz in Figures 2.5 - 2.8 are not present in the non-corrected noise data but are due to frequency dependent variations of the measured transmission loss which probably were different or absent during the ship noise measurements.

"CCGS JOHN A MACDONALD"

Measurements of underwater noise from the icebreaker CCGS JOHN A. MACDONALD has been reported by Thiele /9/ and by Leggat /10/ and



Greene /11/. The 3685 DWT Arctic icebreaker which is owned and operated by the Canadian Coast Guard, is powered by a 11200 kW diesel electric propulsion plant which is connected to three 4 bladed propellers. The 4.1 m diameter fixed, pitch propellers are all located aft in a wing - centre line - wing arrangement. The profile of CCGS JOHN A. MACDONALD is shown in Figure 2.9 below.

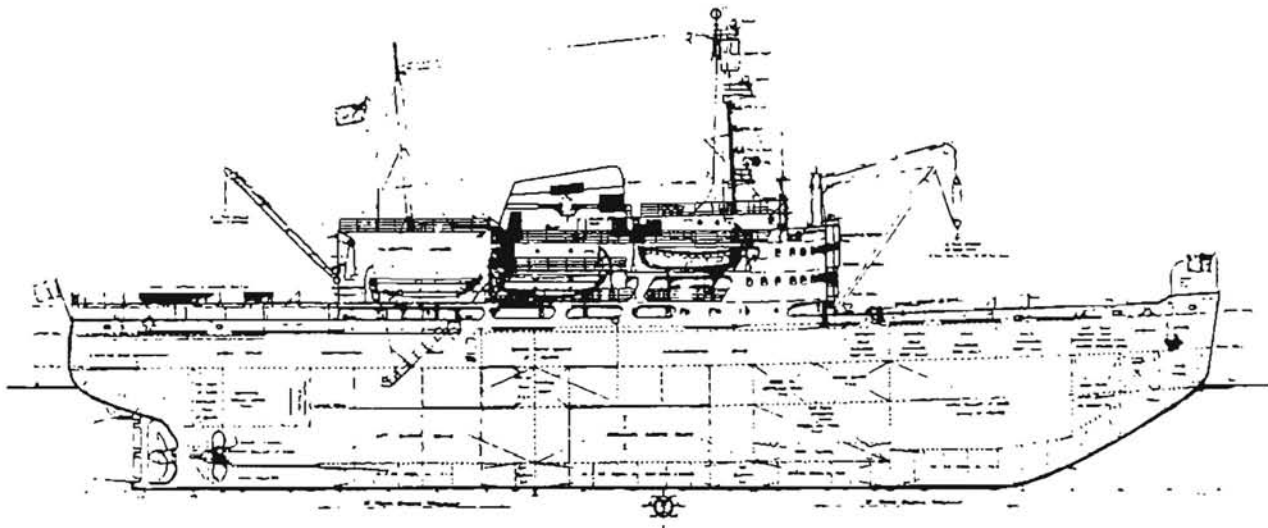


Figure 2.9.
Elevation plan of the Arctic icebreaker CCGS JOHN A.
MACDONALD.

The noise measurements reported by Thiele were made during a passage through the Baffin Bay and Lancaster Sound and provided ship noise data for navigation in pack ice less than 1 m thick and of 5/10 - 8/10 coverage and for navigation in 2.5 m thick fast ice of 10/10 coverage. During the navigation in pack-ice the icebreaker was operating in an ahead condition with changing engine/propeller load according to the local ice concentration whereas navigation in the heavy fast ice necessitated constant ramming operations during which the engine/propeller load changed periodically from full ahead to full astern and idle.



The ship noise recordings were made by means of three omnidirectional hydrophones suspended from the ice at depths of 5 m, 50 m and 100 m below the sea surface. The distance from the icebreaker was monitored continuously and recorded along with the noise data and information about the engine load and the propeller revolutions of the ship. The weather was calm with periods of fog during both series of measurements. The air temperature ranged from 0°C to 5°C below zero.

In the laboratory, the recorded ship noise data were analysed in 1/3-octave bands in the frequency range 25 Hz - 5 kHz and converted to free field source strength referring to 1 m distance by correcting the measured noise levels with the appropriate transmission losses measured at five ranges between the icebreaker and the measuring station. The source level spectrum for each individual load condition was finally obtained as an average of the individual source levels computed for each range for which a transmission loss measurement was available and for each hydrophone depth involved.

The underwater noise measurements reported by Leggat /10/ were conducted on the DREA Halifax Sound Range and provided ship noise data for CCGS JOHN A. MACDONALD sailing in open water. The ship noise was measured by means of a single omnidirectional hydrophone mounted on the sea bottom at a depth of 27 m. The distance between the ship and the hydrophone was monitored continuously during the noise trails.

The ship noise recorded was analysed in 1/1-octave bands in the frequency range 8 Hz - 32 kHz and converted to source levels referring to 1 m distance from the ship by adding an appropriate transmission loss to the analysed data. The transmission loss applied in this case correspond to spherical spreading i.e. $20 \log R$ where R is the range from the ship to the hydrophone.

The measurements reported by Thiele and Leggat cover noise data obtained under a wide variety of ice conditions, engine/propeller



loads, and speeds of advance. The present discussion will however, be limited to ship noise data obtained under comparable engine/propeller loads but under different ice conditions. The particulars of the load/ice conditions treated and the numerical values of the parameters relevant to the prediction models due to Ross and Brown are given in Table 2.3 below.

Load condition No.	Ice Cond.	Eng. load (kW)	Prop. rev. (rpm)	V_t/V_i	A_C/A_D
1. "1/1 power ahead"	Fast ice Pack ice Open water	10900	140	3.0	0.5
2. "1/1 power astern"	Fast ice Open water	10700	140	5.0	0.9
3. "1/4 power ahead"	Pack ice Open water	2500	110	1.5	0.2

Table 2.3.

Particulars of the loading conditions of the CCGS JOHN A. MACDONALD chosen for the comparison of noise data obtained during operation in fast ice, pack ice and open water.

Figures 2.10-2.12 below compare the measured noise level spectra L_S obtained during similar engine load conditions with the source level spectra predicted by the modified Ross model, equations (2) and (3), and the modified Brown model, equations (4) and (6). The numerical values of V_t/V_i and A_C/A_D are not measured but are estimated values based on experience. The measured and predicted source level spectra shown below includes contributions from all three propellers. The predicted source level spectra were obtained by adding the source level spectra from the individual propellers on an energy basis.

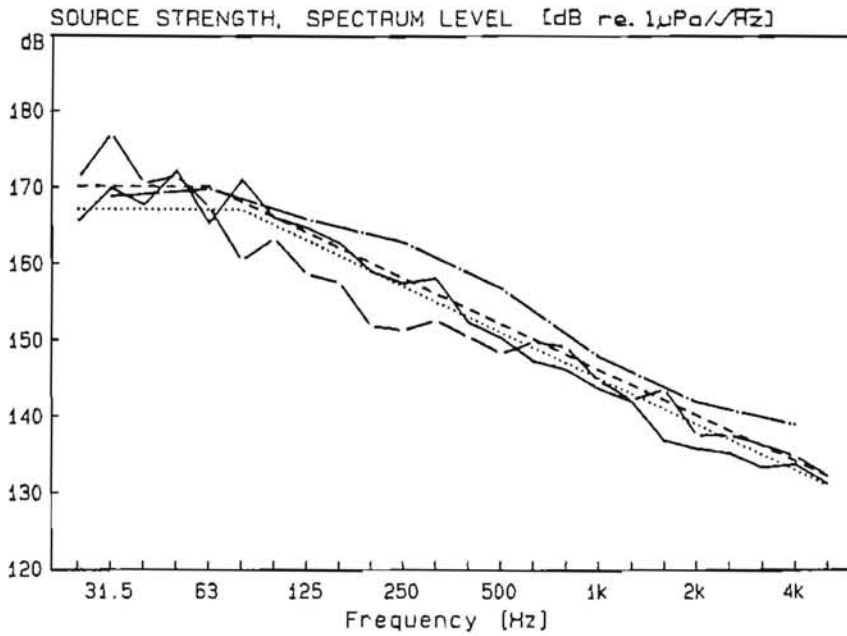


Figure 2.10.

Measured and predicted source level spectra for load condition 1.

Measurements: Fast ice Full, Pack ice ---, Open water ---
Prediction : Ross, Brown -----

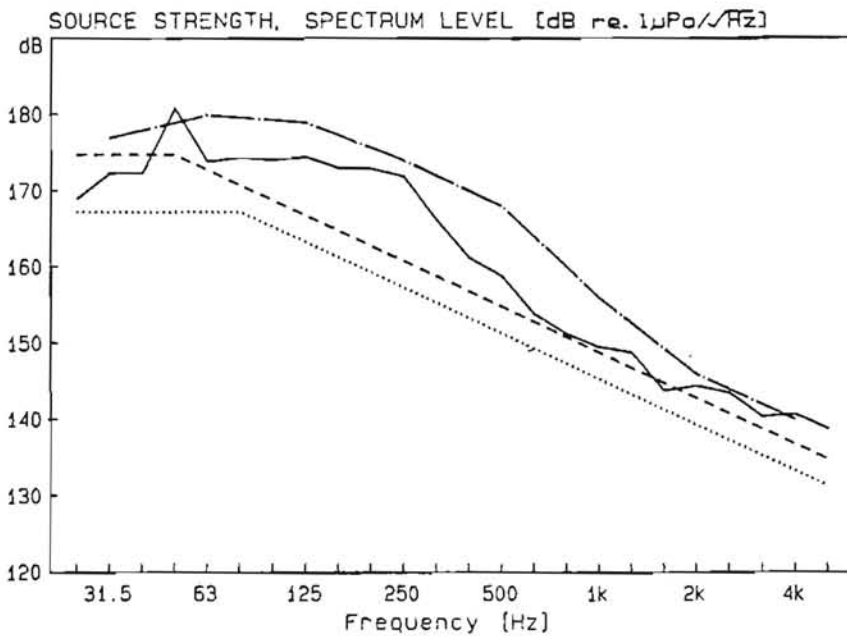


Figure 2.11.

Measured and predicted source level spectra for load condition 2.

Measurements: Fast ice Full, Open water ---
Predictions : Ross, Brown -----

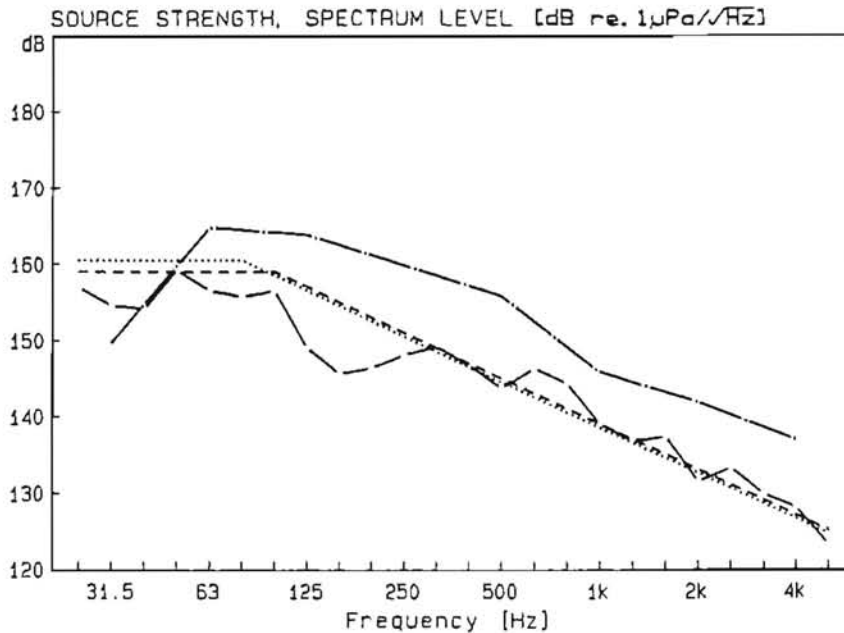


Figure 2.12.

Measured and predicted source level spectra for load condition 3.

Measurements: Pack ice --- , Open water -.-
Predictions : Ross, Brown -----

As seen from Figure 2.10 the modified source level models due to Ross and Brown predict source strength spectra which are in fair agreement with the measured spectra obtained for navigation under three very different ice conditions. The deviation between the prediction and the measurements is 6 dB or less for most of the frequency range investigated. The best agreement between measurements and predictions is obtained for the fast ice condition whereas the measurements obtained for navigation in open water and pack ice are found to be 2-5 dB above or below the predictions, respectively.

The spectrum levels measured during the "1/1 power astern" condition and shown in Figure 2.11 display larger deviations from the predicted spectrum levels than the "1/1 power ahead" data. This



effect is particularly pronounced in the frequency range 80 Hz - 500 Hz where the measurements exceed the predictions by 2-10 dB for the noise data obtained in fast ice and by 4-12 dB for the noise data obtained in open water at the sound range.

A possible explanation for this observed discrepancy is that the prediction models due to Ross and Brown were based on measurements of noise from and cavitation observations of propellers which were assumed to work under normal inflow conditions, an assumption which is invalid under astern operations. When a fixed pitch propeller is operated in astern mode, the trailing edges of the propeller blades become leading edges and the camber distribution becomes reversed relative to the water flow. This situation is likely to change the cavitation performance of the propeller dramatically and thus the noise emission.

In particular the ratio of the tip speed to the inception speed V_t/V_i is expected to change and thus the numerical value of the "break" frequency f_p .

The spectrum levels for the "1/4 power ahead" condition given in Figure 2.12 show a fair agreement between measurements obtained in pack ice and predicted spectrum levels, whereas the open water data exceed the predictions by 4-8 dB in most of the frequency range shown. This tendency for open water spectrum levels to be higher than spectrum levels obtained during navigation in ice, suggests that the "ice breaking process" itself does not contribute significantly to the ship noise measured at a distance. This observation is supported by the data shown in Figure 2.13.

Figure 2.13 compares a time trace of the overall underwater noise level L'_g measured simultaneously at a distance from CCGS JOHN A. MACDONALD with time traces of the overall acceleration level L'_a measured by means of accelerometers mounted on the hull in the bow and on the hull above the propellers of the ship. The time trace of the sound pressure level has been shifted relatively to the acceleration traces in order to account for the time delay caused by the finite propagation time of the sound signal.

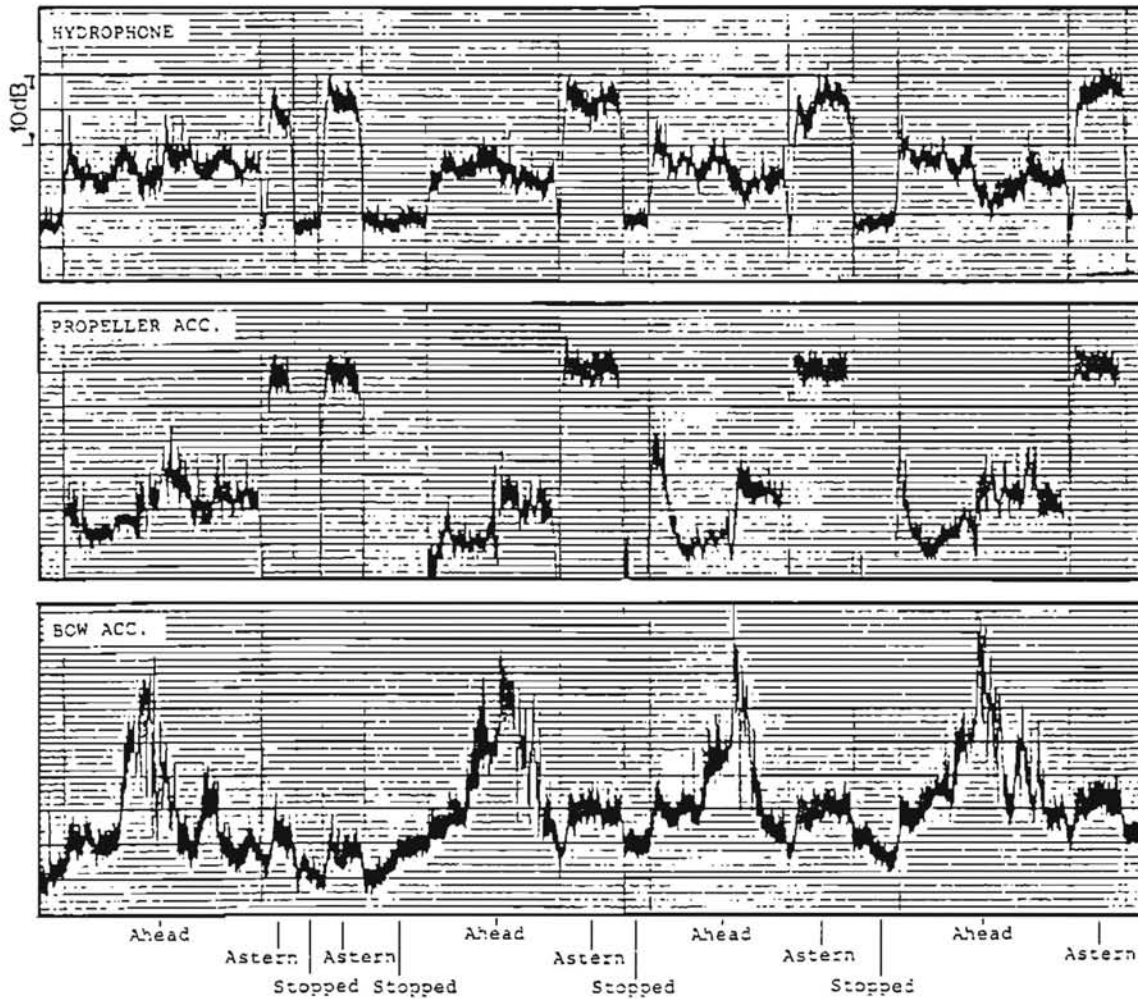


Figure 2.13.

Comparison of underwater noise levels measured at a distance with acceleration levels measured in the bow and stern of CCGS JOHN A. MACDONALD during ramming operations.

As seen from Figure 2.13 the periods of high underwater noise levels coincides with high acceleration levels in the stern of the ship caused by heavy propeller cavitation prevailing in the "astern" condition, whereas periods of high bow acceleration levels induced by ramming and breaking of the ice do not contribute significantly to the underwater noise level at a distance.



3. SOUND TRANSMISSION LOSS

The sea with its boundaries constitutes a complex environment for the propagation of sound. Temperature and salinity variations in the sea water, the sea surface and the sea bottom affect sound propagation in many ways. When travelling through the sea, from a source to a receiver, a sound signal suffers delays, distortions and becomes weakened. The transmission loss TL appropriate to the sonar equation (1) describes one of the effects of sound propagation in the sea, i.e. the magnitude of the weakening of sound between a source and a receiver located at some distant point. More specifically TL is the ratio in decibels between the intensity of the sound signal 1 metre from the acoustic centre of the source and the intensity of the sound signal at the receiver location.

3.1 Sound Propagation in a Homogeneous Sea

The Transmission Loss quantity TL entering the sonar equation may be considered to be the sum of two physically different loss mechanisms, the spreading loss SL and the attenuation loss AL

$$TL = SL + AL \quad (7)$$

The spreading loss SL is a geometrical effect representing the regular weakening of sound as a signal spreads out from the source.

In a homogeneous, unbounded medium without attenuation losses, sound is radiated equally in all directions and becomes equally distributed over concentric spheres surrounding the source. In this case the sound intensity decreases as the square of the range R, and the spreading loss may be found according to the law of spherical spreading

$$SL = 20 \log R \quad (8)$$



Spherical spreading is often found to be a good approximation to the transmission loss encountered in the ocean at short ranges typically at distances shorter than ten times the water depth.

If the medium in which the sound propagates is bounded by two plane parallel boundaries, as the sea is, spherical spreading cannot take place beyond a certain range. The sound will now be radiated parallel to the boundaries and will become equally distributed over co-axial cylindrical surfaces of equal height. In this case the sound intensity decreases with the first power of the range R and the spreading loss may be found according to the law of cylindrical spreading

$$SL = 10 \log R \quad (9)$$

Cylindrical spreading is often found to be a good approximation to the transmission loss encountered in the ocean at long ranges typically an order of magnitude longer than the water depth.

The attenuation loss AL covers a number of different physical processes other than geometrical spreading by which sound becomes attenuated when propagating in the sea. Important mechanisms constitute absorption of sound in the water, non-coherent scattering at the bottom and sea surface and leakage of sound from the body of water into the subsurface. The attenuation loss is found to vary linearly with distance and is expressed as a certain number of decibels per unit distance i.e.

$$AL = aR$$

The quantity " a " termed the logarithmic attenuation coefficient is in general found to be a function of frequency but for open ocean environment it is commonly assumed to be constant at frequencies below 200 Hz and obtain numerical values in the range $2 \cdot 10^{-3}$ dB/km $<a<$ $2 \cdot 10^{-2}$ dB/km depending on the particular ocean environment. Reference is made to Mellen, Browning and Ross /12/.



For frequencies above 200 Hz the logarithmic attenuation coefficient "a" is found to increase as frequency squared in accordance with the theory due to Thorp /13/. The low values of the logarithmic attenuation coefficient given above indicate that propagation of the dominating low frequency part of ship noise spectra is governed mainly by geometrical spreading.

3.2 Sound Propagation in Arctic Waters

Sound propagation in a real ocean is far more complex than it may appear from the previous section. Changes in the sound velocity as a function of depth, the roughness of the sea surface and the acoustic properties of the sea floor are important factors which may influence the sound propagation and thus change the transmission loss calculated from expressions which assume a homogeneous ocean bounded by plane reflecting surfaces.

In Arctic waters the sound velocity attains its minimum value close to the sea surface and is found to increase with increasing depth. This condition will prevent noise emitted from a surface ship to spread in a homogeneous way throughout the body of water but will cause the sound waves to be distributed unevenly over the water column or to be trapped in a sound channel located just below the sea surface.

The situation is illustrated in Figures 3.1 and 3.2 which show ray-trace diagrams calculated utilizing sound velocity profiles measured at two locations in Baffin Bay and Lancaster Sound by Thiele /9/. The left parts of the diagrams display the sound velocity in m/sec. versus depth in metres. The right parts of the diagrams map out the sound rays which are representatives of the path propagating sound waves following a vertical plane in the ocean. The source which is located at a depth of 4 metres below the sea surface is situated on the depth axis at 0 metres distance.

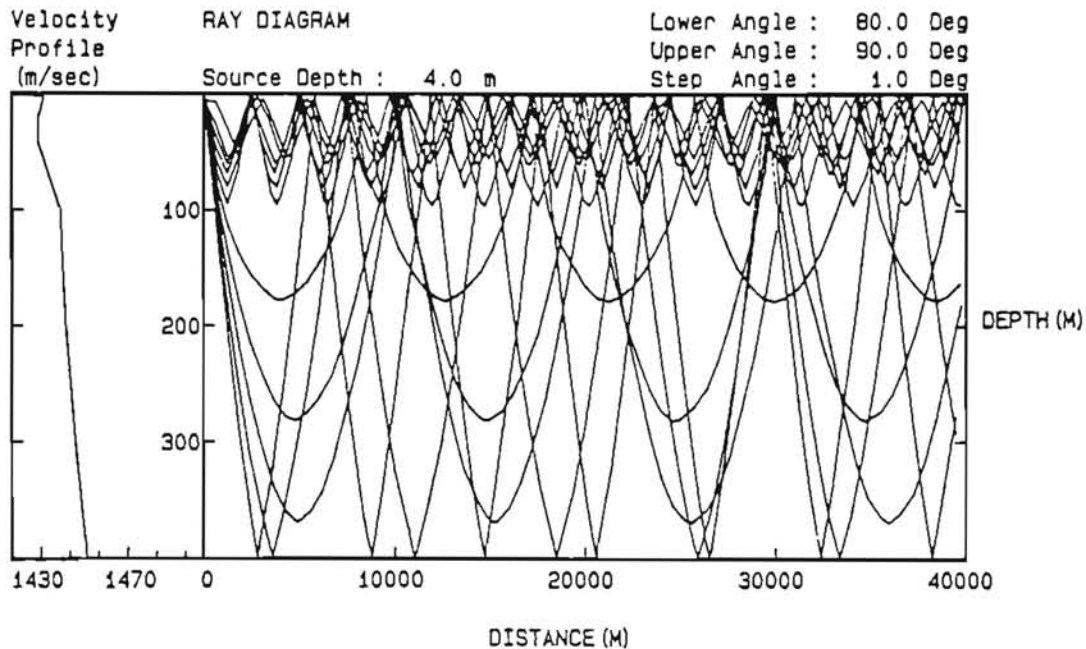


Figure 3.1.
Ray-trace diagram of the sound field corresponding to the sound velocity profile measured at a location in Baffin Bay. Source depth: 4 metres.

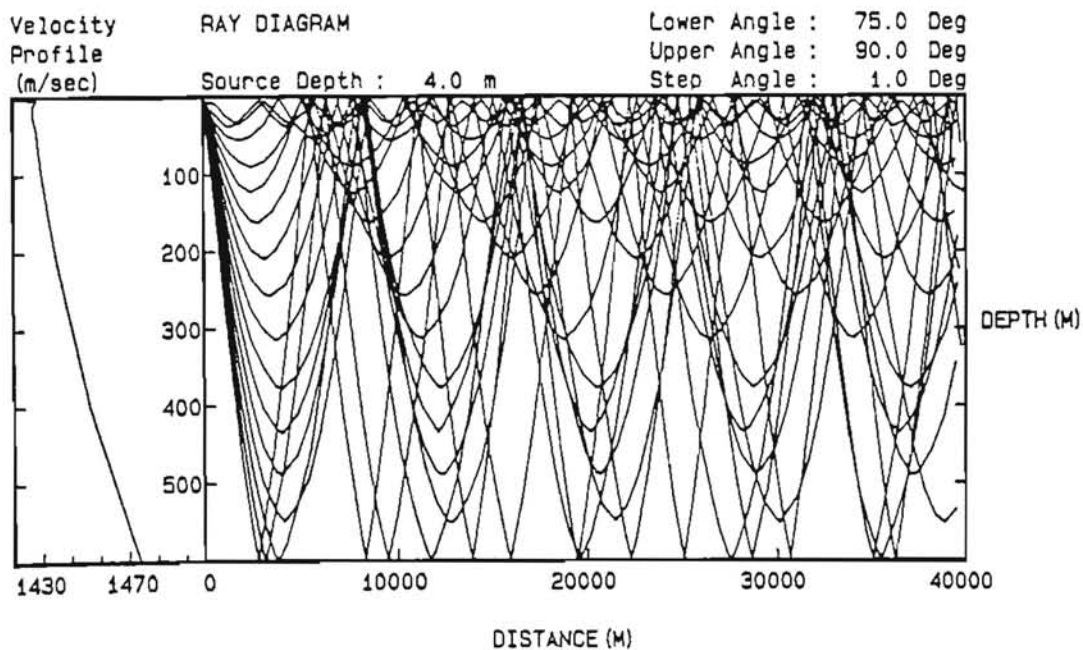


Figure 3.2.
Ray-trace diagram of sound field corresponding to the sound velocity profile measured at a location in Lancaster Sound. Sound depth: 4 metres.



From Figure 3.1 it is observed that most of the rays are confined to a horizontal layer extending from the sea surface to a depth of approximately 100 metres. This layer forms a sound channel in which most of the noise emitted by a surface ship will propagate, governed by successive upward refractions due to the positive sound velocity gradient and downward reflections from the sea surface. Formation of this sound channel is associated with the strong positive sound velocity gradient found in the depth range 40-100 metres.

Below the sound channel the rays are less dense than in the channel, indicating that sound waves propagating from the shallow source to a deep receiver suffer a relatively large geometrical spreading loss as compared with sound waves which propagate to a receiver located in the sound channel.

The ray-trace diagram given in Figure 3.2 does not reveal formation of a distinct shallow sound channel as does Figure 3.1. The presence of a smoothly increasing sound velocity profile with depth does, however, ensure upward refraction of down going sound waves and thus cause a major part of the acoustic energy to be propagated to a distance via the surface reflected path. The density of the sound rays are seen to be almost constant throughout the water column, hence sound waves propagating from the shallow source to a deep receiver are expected to suffer approximately the same geometrical spreading loss as sound waves which propagate to a shallow receiver.

Besides the prevailing positive sound velocity gradient, the ice cover constitutes a boundary condition which has a pronounced effect on sound propagation in the Arctic waters whenever it is present. The ice/water boundary is mostly found to be very irregular and rough. As a consequence, incident sound waves are scattered in all directions leading to large reflection losses for the under ice condition. This situation is quite different from the open water conditions for which sea surface reflection losses are found to be quite small.



In conclusion the key features of sound propagation in the Arctic sea may be characterized as follows:

Sound transmission in the Arctic waters is mainly governed by upward refracted surface reflected sound propagation. Thus the acoustic properties of the sea floor are of minor importance as compared with the acoustic properties of the air/water or ice/water boundary. Generally speaking the sound transmission loss in the Arctic waters is less than in other waters when open water conditions prevail but larger when an ice cover is present.

3.3 Prediction Models

In order to determine the sound propagation and the influence of various effects, a number of prediction models have been developed. Models for prediction of the sound transmission loss can be divided into three groups:

- 1) Empirical.
- 2) Analytical.
- 3) Numerical methods.

There are a number of different methods, each with advantages and disadvantages. In this report, however, only the most commonly used methods will be described.

Empirical Methods

Empirical methods are based on statistically treated data obtained by measurement.

Most empirical transmission loss prediction models are based on the relations described in Section 3.1. Cylindrical or spherical spreading is assumed, depending on the range, and the attenuation coefficient is left to be determined. This has to be done by means of measurements. In order to obtain values at low frequen-



cies the measurements must be performed at long ranges as the magnitude of non-spreading losses per unit distance diminishes with decreasing acoustic frequency. The discussion of mechanisms contributing to the attenuation loss is given in Section 3.1.

Analytical Methods

The analytical and the numerical prediction models have in common that they offer solutions for the wave equation. The wave equation is a partial differential equation which describes the propagation of sound waves. Basically, analytical solutions can be obtained by hand, often however, a computer programme is used.

One form of solution is provided by normal mode theory. In normal mode theory, the sea and the sea floor are divided into stratified layers in which the sound velocity and density are assumed to be constant. The solution is divided into modes describing the sound pressure versus depth for the individual modes. An example is given in Figure 3.3. The sum of the modes forms the solution which within the assumption made, is a complete solution. Except in the simplest problems, the normal mode theory requires a computer programme in order to handle the range of stratified layers and boundary conditions that can be expected in a real problem.

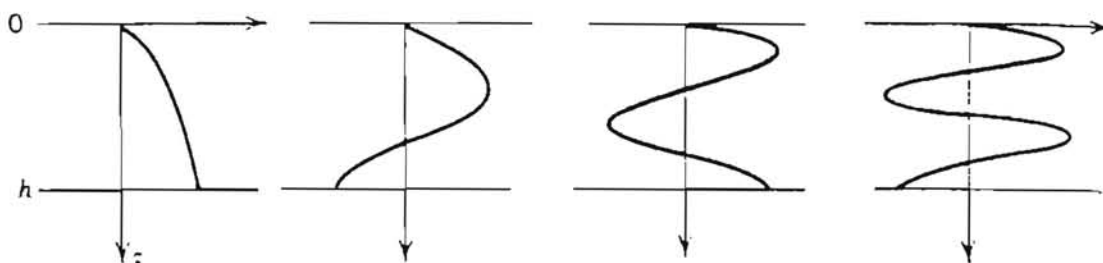


Figure 3.3.
Sound pressure versus depth for the first four modes of
a normal mode solution. Reference /22/.



The normal mode method is valid at all frequencies but in practice most useful at low frequencies and in shallow water where only few modes are present. For further information see Clay and Medwin /22/ and Tolstoy and Clay /23/.

Another form of the solution to the wave equation is provided by ray theory. An important result of the ray theory is Snell's law which describes the relation between sound velocity and propagation. By Snell's law the sound propagation can be visualized by rays that describe where to in space sound emanating from the source is propagating. These rays are not frequency dependent. Using the ray theory for drawing ray diagrams is called ray tracing. Examples of ray tracing have been shown previously in Figures 3.1 and 3.2. Ray diagrams can be drawn by hand, normally though a ray trace computer programme is used. Ray tracing provides an easily interpreted picture of the sound propagation which, however, is subject to some drawbacks. Most seriously are the restriction of only being valid at high frequencies and that certain special cases of propagation cannot be treated. Reference is made to Clay and Medwin /22/ and Tolstoy and Clay /23/.

Numerical Methods

Numerical methods solve the wave equation by an iterative process. In order to get a sufficiently accurate result, a large number of iterations is needed and this is practicable only on a computer.

Two numerical methods named the Fast Field Programme (FFP) technique and the Direct Global Matrix (DGM) technique are presented in this section.

Basically the concept and the output of these two methods is the same, the major difference being that the DGM method calculates the sound propagation in 3 dimensions and hence with a better accuracy than the FFP method which calculates in 2 dimensions. In both methods the wave equation is rewritten into a form which can



be solved numerically by means of a Fast Fourier Transformation. The sea and the sea bottom are divided into stratified layers. Calculations with fine accuracy can be obtained with these methods if a proper description of the material parameters of each layer is available. An example of a transmission loss by the DGM is shown in Figure 3.4. The transmission loss is shown as a function of frequency but can also be shown as a function of range.

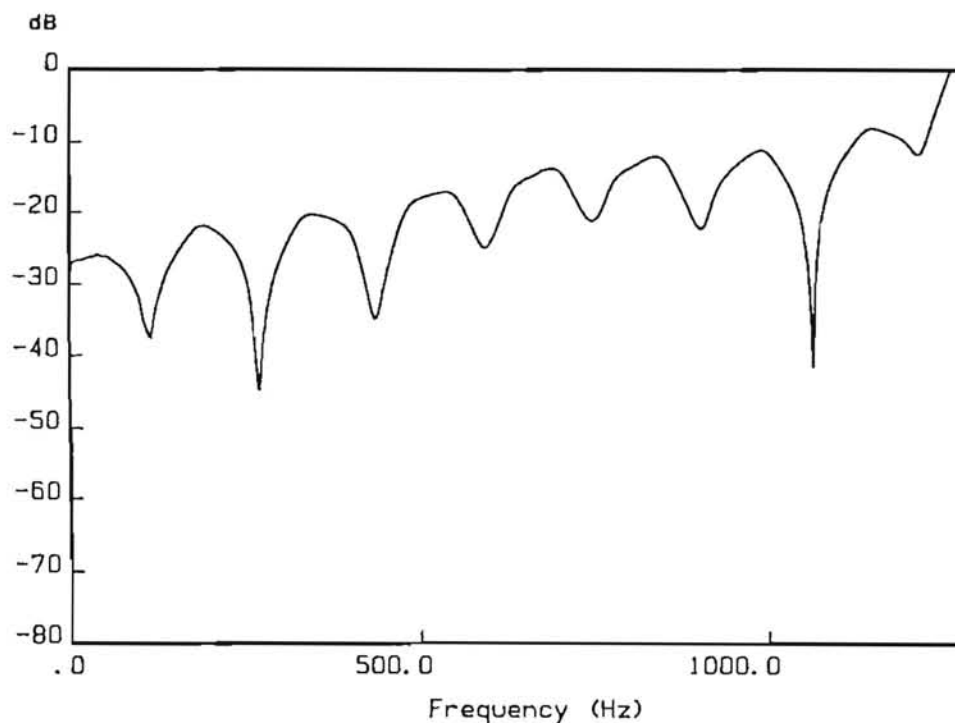


Figure 3.4.
Example of transmission loss versus frequency calculated by the DGM method. Calculated for source at 1 metre and receiver at 9 metres at short range.

Within the major concept different approaches have been developed in order to make the computations as fast and efficient as possible. For the FFP method further information can be acquired Rasmussen and Vistisen /24/ and for the DGM method from Vilmann et al. /25/.



3.4 Transmission Loss Measurements

Information about the exact sound transmission loss in a specific position can be obtained by measurements. In this way all factors affecting the sound propagation in the actual area have been taken into account.

The measurements described in reference Thiele /9/ have been carried out by means of small explosive charges used as sound sources. The transmission loss can be determined as the difference between the pressure level measured at a source hydrophone close to the explosive charge and a receiver hydrophone placed at varying distances. The pressure level of the source hydrophone is corrected for bottom and surface reflections so that the signal can be considered as the free field pressure level. In Figure 3.5 is given an example of the measured transmission loss in Baffin Bay and Lancaster Sound.

During the measurements in Baffin Bay the area was dominated by pack ice with some open water areas and some large floes. The ice thickness was less than 1 metre. The water depth was approximately 400 metres. At Lancaster Sound there was shore fast ice with a thickness of approximately 2.5 metres with few ridges. The water depth was approximately 600 metres, Thiele /9/.

The transmission loss obtained by measurements includes, as mentioned above, all aspects of the sound propagation but is only valid for the specific measurement position and for the specific source and receiver depths used during the measurement.

Figure 3.6 shows a comparison between a measured transmission loss and the corresponding transmission loss calculated numerically by the DGM method. The example has been taken from Thiele /9/.

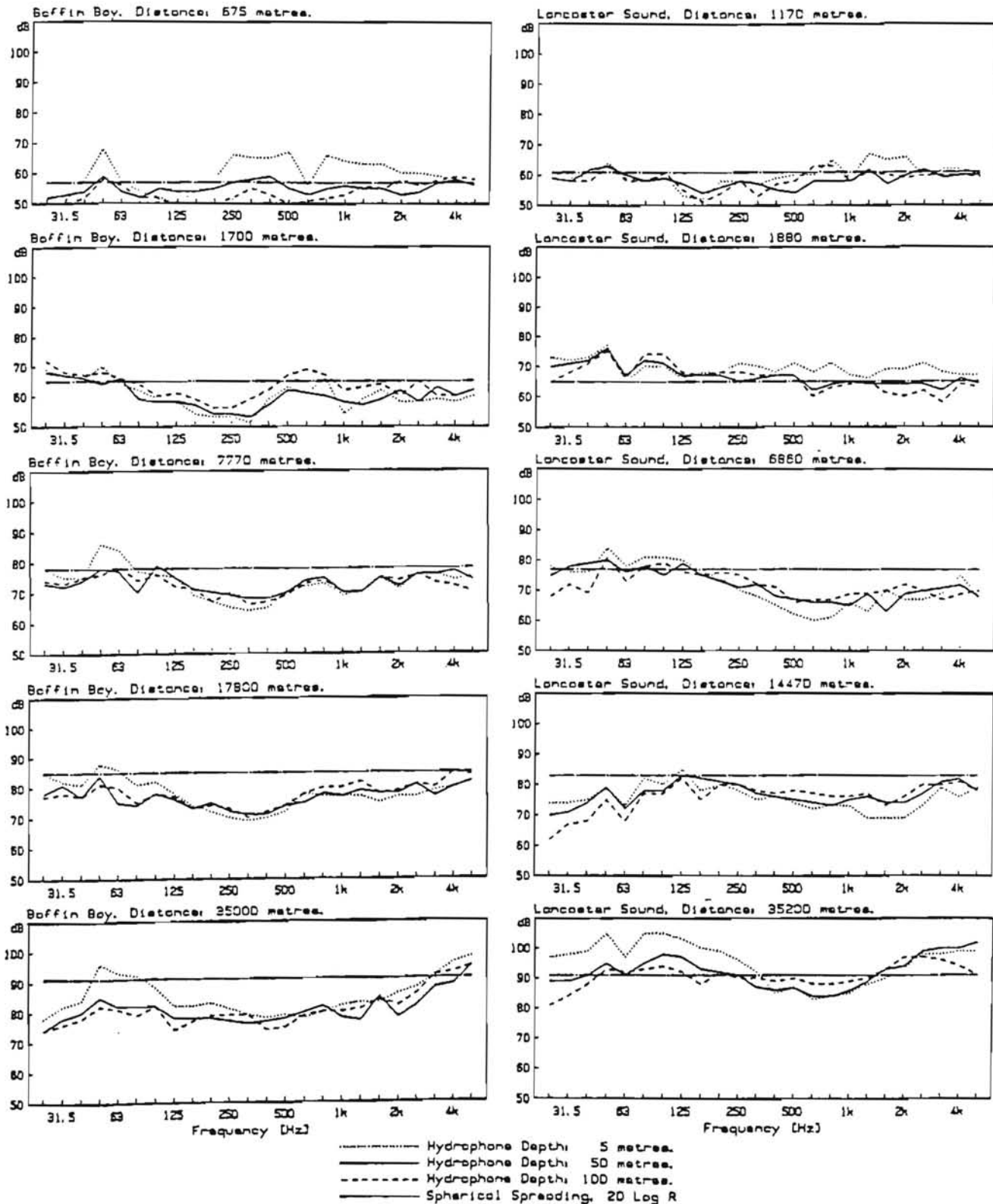


Figure 3.5.
Measured average transmission loss per 1/3-octave frequency bands measured in Baffin Bay (left side) and in Lancaster Sound (right side). Taken from Thiele /9/.

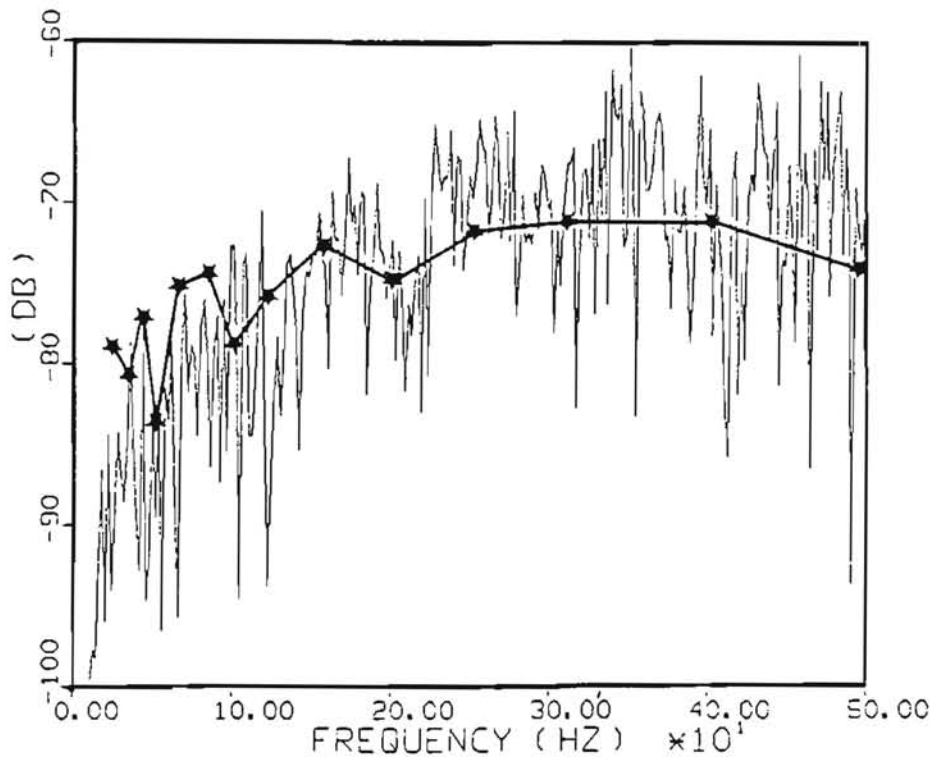


Figure 3.6.
Sound transmission loss calculated by the DGM method for Baffin Bay conditions at a distance of 18 km. The losses actually measured in 1/3-octave are marked with *-*-. Thiele /9/.

For a more detailed description of the transmission loss measurements and signal analysis reference is made to Thiele /9/.

3.5 Suggested Transmission Loss Models for Noise Exposure Modeling

In the noise exposure programme described in Section 5 a transmission loss is required as input. It has been chosen that the transmission loss is to be given as a table of data values at a number of fixed ranges. The data values can either be calculated from one of the detailed prediction models or it can be measured data. In order to obtain transmission losses when no data are available or when ranges are exceeding the data available, it is chosen to use an empirical determination of transmission loss. An empirical model provides a fast and efficient prediction of the



transmission loss. Analytical and numerical methods might provide a more exact estimate but in order to cover the wide spread area which was to be treated in the noise exposure model, these methods would have demanded a vast amount of calculations.

The transmission loss can be written in an empirical form as:

$$TL = H_0 + 10 \log R + aR \times 10^{-3} \quad (10)$$

H_0 accounts for the spherical spreading close to the source, $10 \log R$ is the cylindrical spreading with R in metres and "a" is the attenuation, dB/km, due to effects other than spreading. In this form (10) can be used at both ranges close to the source where spherical spreading is assumed and at large ranges where cylindrical spreading is assumed. The range R_0 where channelling becomes dominant is empirically set to be:

$$R_0 = 225 \sqrt{H} \quad (11)$$

where H is the water depth or sound channel depth.

At ranges shorter than R_0 , H_0 is set equal to $10 \log R$ so that (10) becomes

$$TL = 20 \log R + aR \times 10^{-3} \quad (12)$$

At ranges larger than R_0 , H_0 is set equal to $10 \log R_0$ and as such represents the loss in excess of cylindrical spreading incurred at ranges less than R_0 . By combining equation (10) and (11) the transmission loss becomes

$$TL = 5 \log H + 23.5 + 10 \log R + aR \times 10^{-3} \quad (13)$$

In order to utilize equations (12) and (13) the attenuation coefficient "a" must be known. The determination of "a" is based on an empirical method by Thorp /13/ who has studied the attenuation due to absorption.



In the low frequency region attenuation due to scattering becomes important. Scattering effects have been investigated in open water conditions in Baffin Bay by Mellen, Browning and Ross /12/ and during ice conditions in the East Greenland Sea by Diachock /26/. The results from these references have been curve fitted and the resulting attenuation coefficients due to scattering have been included in the model by Thorp. Additional effects of sound leakage from the sound channel is included in open water conditions after a model by Baker /27/. The leakage coefficient depends on the frequency, the sea state, S, and the water or sound channel depth, H_0 .

The total attenuation coefficient can be written as:

Open Water

$$a = \frac{0.022 f^4}{0.0009 + f^4} + \frac{0.11 f^2}{1.0 + f^2} + \frac{43.7 f^2}{4100 + f^2} + \frac{0.76 f}{\sqrt{H}} \times 1.4^S \quad (14)$$

Under Ice

$$a = \frac{0.235(f)^3}{0.0023 + (f)^3} + \frac{0.11(f)^2}{1.0 + (f)^2} + \frac{43.7(f)^2}{4100 + (f)^2} \quad (15)$$

f is the frequency in kHz,

a is attenuation loss in dB/km.

By properly combining the equations (12), (13), (14) and (15) an estimate of the sound transmission loss can be found.



4. AMBIENT NOISE IN THE SEA

Ambient noise in the sea may be defined as the noise background at a particular location against which a certain desired sound signal must be detected. Ambient noise may possess certain directional characteristics depending on the sources of the noise and the topography of the sea floor.

However, for the present purpose the ambient noise level L_a appropriate to the sonar equation (1) will be defined as the intensity in decibels of the ambient background measured by an omnidirectional hydrophone and referred to the intensity of a plane wave having an rms pressure amplitude of 1 uPa. Although ambient noise spectra may be measured in different frequency bands the ambient levels L_a given in the present report are always given as spectrum levels reduced to a 1 Hz frequency band.

4.1 Sources of Ambient Noise in Arctic Waters

The waters of the Arctic region is a unique noise environment mainly due to the presence of the ice. The ambient noise levels measured in this region are highly variable on a seasonal basis as well as on a short term basis, and are usually found to originate from dynamic processes caused by the ice. This situation is different from the situation found in ice free waters in other parts of the world where the ambient noise originates from wind agitation of the sea surface, from rain and spray impacts and from distant shipping. Reference is made to Urick /14/.

In areas characterized by a continuous fast ice cover, the dominating source of ambient noise is the ice cracking induced by thermal stresses. The cracks occur near the surface of the ice and are the result of radiative cooling during periods of falling air temperature. The spectrum of cracking noise typically displays a broad maximum in the decade from 100 Hz - 1.0 kHz and the spectrum level has been observed to vary as much as 15 dB within 24 hours due to the diurnal change of air temperature, see reference /15/.



During periods in which cracking noises are absent, noise, generated by the wind flow and snow drift over the rough ice surface, is found to dominate the ambient noise spectrum. The noise spectrum generated by the wind is found to be flat in the frequency range 100 Hz -10 kHz with a spectrum level determined by the wind speed. In the absence of cracking and wind noises, areas covered by shore-fast ice are known to be one of the quietest underwater environments in the sea.

In regions off-shore, the ice cover rarely becomes shore-fast but will be kept in constant movement by currents, the wind and the tide. Forces exerted on the ice by the wind and currents will cause cracks and ridges to form and the rubbing, bumping and piling up of the ice masses involved are known to be a major source of ambient noise.

During the summer period, large areas of the Arctic sea surface will be free of a continuous ice cover but drifting ice floes and icebergs are usually scattered at irregular intervals. The melting, collisions, breaking up and turning over of these ice formations constitute major sources of ambient noise in the Arctic sea during the summer. During melting of ice the steady release of air bubbles contained under pressure gives rise to underwater noise. The noise spectrum is found to be flat up to about 10 kHz and the level is often so high that it dominates the ambient noise in locations where melting ice formations occur. The breaking up and turning over of icebergs are known to generate strong pulses of underwater sound. Such pulses will, in conjunction with sound emitted by the interaction between the bottom and drifting icebergs, constitute major sources of ambient noise in the Arctic sea during summer periods.

The marginal ice zone, i.e. the region in vicinity of the edge of large sheets of ice, is usually characterized by quite high levels of ambient noise as compared with other areas in the Arctic sea. The impact of waves against the ice edge is a major source of ambient noise but also the breaking up and rafting of ice



floes contribute significantly to the ambient noise in this region. Measurements made in the marginal ice zone have revealed that the ambient noise beneath the ice edge may be 4-12 dB higher than in open water at the prevailing sea state and as much as 10-20 dB higher than the noise level to be measured under the continuous ice cover, see reference /17/.

Apart from the ice, other sound sources may influence the ambient noise in Arctic waters. In regions of open water, noise due to wind agitation of the sea surface is significant. Furthermore, biological noise in the form of sounds emitted by marine mammals, fish and shellfish may contribute to the ambient noise level in the Arctic sea and in particular to the ambient noise of the marginal ice zone.

4.2 Measurements of Ambient Noise in Arctic Waters

In order to establish ambient noise standards suitable for noise exposure modelling, the existing unclassified literature on ambient noise in Arctic waters has been reviewed. This survey revealed that only a few investigations of ambient noise in the Baffin Bay/Davis Strait region have been published prior to the start of the APP project and the majority of this material was concerned with sites off the Canadian Arctic coast, the Parry Channel or in the central part of the Baffin Bay. Hardly any ambient noise measurements appeared to have been made off the north west coast of Greenland.

The ambient noise measurements reported by Milne and Ganton /15/ were conducted in the Parry Channel and the Beaufort Sea under a 10/10 cover of pack ice during winter and summer periods. During the winter measurements the ice was shore fast whereas it was free to move during the summer measurements. All measurements were made by means of bottom mounted hydrophones. The general findings of these investigations prove that ambient noise in Arctic waters are highly variable and are related to the mechanical process such as cracking, rafting and grinding, occurring within the ice cover.



The ambient noise spectra recorded during summer conditions resemble typical ambient noise spectra obtained in open shallow water areas at sea state 0. Below 125 Hz the individual spectra are almost flat indicating an ambient noise level in the range 54-64 dB/Hz^{1/2} re. 1 uPa. Above 125 Hz the measured spectra roll off at a rate of approximately -5 dB/octave in accordance with the now classical "Knudsen Curves" /16/ which establish a relation between ambient noise in the sea and the prevailing sea state. Reference is made to Figure 4.1 below.

The ambient noise spectra recorded during winter conditions are found to be highly variable as compared with summer conditions revealing distinct noisy and quiet periods. During noisy periods the measured noise spectra closely resemble that of "Knudsen sea state 3", at frequencies down to 125 Hz. Below this frequency the noise spectra are flat corresponding to an ambient noise level of approximately 80 dB/Hz^{1/2} re. 1 uPa. During quiet periods the measured ambient noise spectra fall considerably below "Knudsen sea state 0" for frequencies below 500 Hz, whereas a slight exceeding of this curve is found for frequencies above 500 Hz. Reference is made to Figure 4.2 below.

Ambient noise measurements performed by Diachok and Winokur /17/ were conducted in the marginal ice zone in east Greenland waters during the summer period. The measurements were made by means of hydrophones suspended from 7 sonobuoys at a depth of 30 m and dropped at 28 km intervals along a line perpendicular to the ice edge. The main result of this investigation shows that the ice - open water boundary acts as a line source of noise with noise levels near a well defined ice edge that are about 12 dB higher than open water levels and about 20 dB higher than noise levels far under the ice cover. Measured ambient noise levels near an irregular and diffuse ice edge were about 4 dB higher than those for open water and about 10 dB higher than the noise levels far under the ice field.



The authors related the relatively high ambient noise levels measured near the ice edge to the wave action against the ice edge and interaction between individual floes of ice. Ambient noise spectra estimated from the measurements of Diachok and Winokur display the characteristic -5 dB/octave slope predicted by the "Knudsen Curves" and support the evidence that ambient noise levels below an ice field are significantly lower than open water noise levels. Reference is made to Figure 4.1.

In a volume of workshop proceedings /18/ Leggat, Merklinger and Kennedy have summarized the results of more than 30 observations of ambient noise made during summer periods in the central Baffin Bay and Lancaster Sound when these waters are comparatively ice free. A detailed account of the measured spectra, hydrophone depths and prevailing ice conditions and sea states are not given, leaving only upper and lower limiting envelopes of the measured ambient noise data. As seen from Figure 4.1 the reported ambient noise levels are surprisingly high when compared with the measurements of Milne and Ganton /15/ or Diachok and Winokur /17/.

The upper noise level envelope of Leggat et al. is found approximately to coincide with the "Knudsen Curve" for sea state 6 at frequencies above 125 Hz and tend to be flat for frequencies below 125 Hz. The lower noise level envelope approximates the "Knudsen Curve" for sea state 1 and tends to form a plateau at frequencies below 125 Hz. The high noise levels reported in this ambient noise survey were estimated by Leggat et al to originate from mechanical processes within icebergs and floes of ice which are present even during summer conditions.



The limited amount of ambient noise data available for the Baffin Bay/Davis Strait region initiated a series of ambient noise measurements made by Ødegaard & Danneskiold-Samsøe ApS as consultants to the Greenland Fisheries and Environment Research Institute and the Greenland Technical Organization. The results of these investigations are presented by Thiele in three separate reports /19/, /20/ and /21/ which cover ambient noise measurements made at various geographical locations and different ice conditions.

The measurements reported by Thiele /19/ are concerned with ambient noise in the sea off Scoresbysund, east Greenland during summer conditions. The measurements were made in 5 positions at various distances from the edge of an ice field with a coverage of 4/10 to 7/10 by means of a hydrophone suspended at a depth of 50 m from a dinghy. The weather conditions were calm with winds below 1 m/s and currents less than 0.5 knots. The sea state was estimated to be 0-1/2. The main results of this series of measurements show that the ambient noise varies considerably with time and location, although no correlation with distance to the ice edge was noted.

Analysis of the ambient noise recordings reveals that the noise is composed of frequent transient sound pulses resembling thunder and a continuous hiss, similar to rain noise, sounds which may be attributed to the breaking up of ice formations and to the escape of air bubbles when they are released from the melting ice. Upper and lower envelopes of the measured ambient noise spectra are given in Figure 4.3 which also compare the present measurements with those of Leggat et al /18/. The limiting envelopes are characterized by a broad hump ranging from 68 dB to 80 dB re. $1 \mu\text{Pa}/\text{Hz}^{1/2}$ at frequencies below 500 Hz. At high frequencies the envelopes start to roll off, slowly at first until a limiting slope at approximately -10 dB/octave is reached at 2000 Hz.

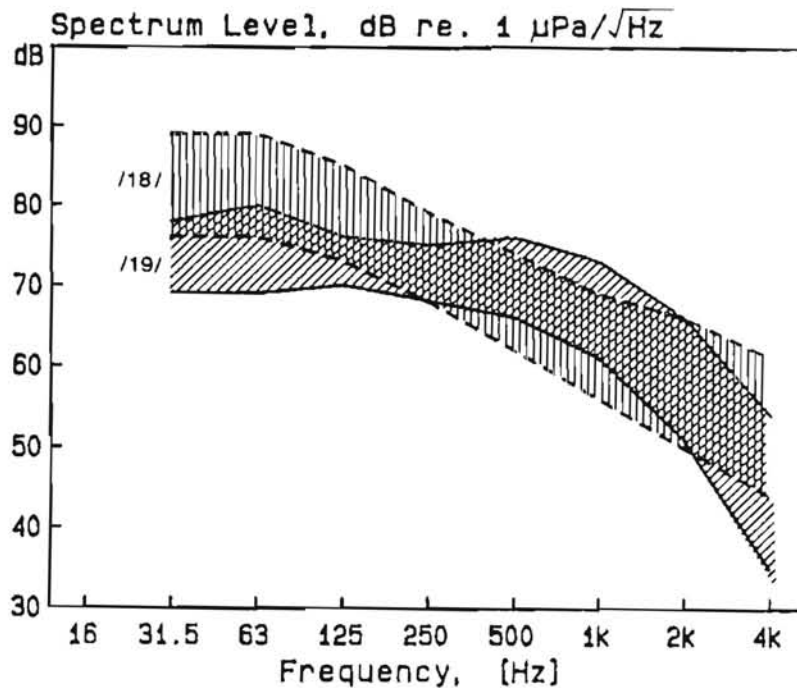


Figure 4.3.

Envelopes of ambient noise spectra measured off Scoresbysund, Thiele /19/ during summer conditions as compared with data for Baffin Bay, Leggat et al. /18/. Noise levels in dB re. $1 \mu\text{Pa}/\text{Hz}^{1/2}$.

As seen from Figure 4.3 the Scoresbysund measurements agree fairly well with the ambient noise data given by Leggat et al. /18/ for frequencies above 250 Hz. At lower frequencies the upper envelope given by Leggat et al exceeds the upper envelope of the Scoresbysund data by as much as 10 dB.

The second series of ambient noise measurements reported by Thiele /20/ were made in the sea off Kap York, north west Greenland, during winter conditions. The measurements were made at 3 different geographical locations by means of a 50 m deep hydrophone suspended through holes drilled in the ice. The weather conditions were calm with winds in the range 0-5 m/s. The ice conditions were characterized as shore fast ice, consolidated pack ice and drifting pack ice.



The main results of these measurements once again emphasize the variable nature of Arctic ambient noise, and support the experience that ambient noise levels measured under a large ice cover are of significantly lower levels than ambient noise levels obtained in open water during summer periods. Analysis of the Kap York measurements reveals that the noise is dominated by relatively loud sound bursts superimposed on a fairly low level constant background. Upper and lower limiting envelopes of the measured ambient noise spectra are given in Figure 4.4 together with the ambient noise data obtained by Leggat et al during summer conditions in the Baffin Bay and the ambient noise data given by Milne and Ganton /15/ valid for the Parry Channel.

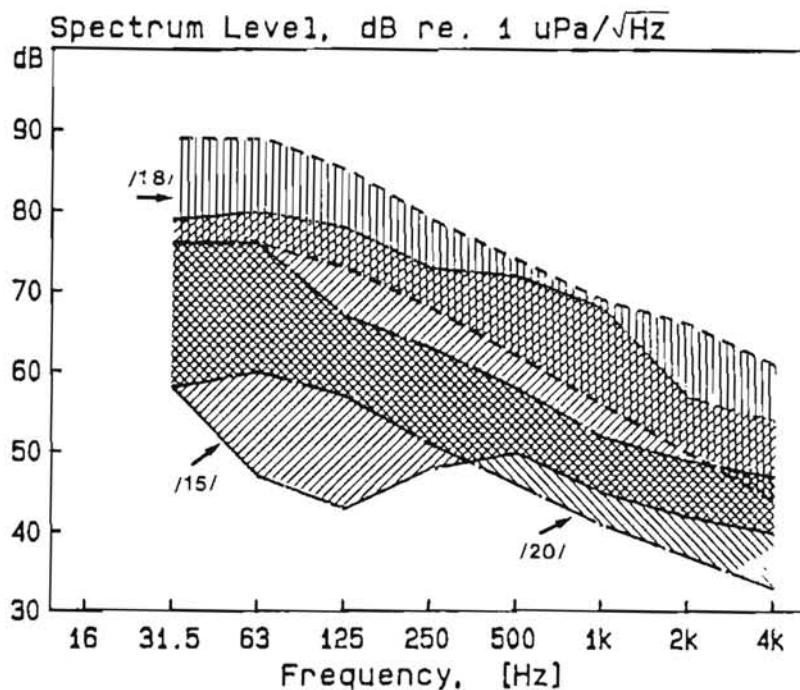


Figure 4.4.

Envelopes of ambient noise spectra measured off Kap York, Thiele /20/ during winter conditions as compared with data obtained in Baffin Bay, Leggat et al. /18/ during summer and in Viscount Melville Sound, Milne and Ganton /15/ during winter. Noise levels in dB re. $1 \mu\text{Pa}/\text{Hz}^{1/2}$.



As seen from the figure above the agreement between the Kap York data and those reported by Milne and Ganton is rather good, the differences being that the Kap York data exceed the levels measured by Milne and Ganton at frequencies below 125 Hz, whereas Kap York data are somewhat lower at the high frequencies. If the Kap York data are compared with those of Leggat et al /18/ it is found that the general shape of the limiting envelopes are quite alike but that the level of the upper and lower envelopes of the data given by Thiele are 10-15 dB lower, emphasizing the relatively quietness of the underwater environment during winter conditions. The slope of the limiting envelopes is approximately -5 dB/octave for frequencies above 125 Hz, below which the noise envelopes have a tendency to be flat.

In order to investigate more thoroughly the effects of seasonal changes in the ice cover on the ambient noise, Thiele /21/ conducted a series of ambient noise measurements during summer conditions in the sea off Thule, north west Greenland, somewhat north of the locations chosen for the Kap York measurements. Most of the measurements were made in open water at various distances from the coast line by means of a 50 m deep hydrophone suspended from a dinghy. Additional measurements were made by means of a 5 m deep hydrophone in order to quantify the effects of hydrophone submergence.

The weather conditions were reported to be relatively calm with winds in the range 0-5 m/s and sea states ranging from 0-1/2. The ice conditions ranged from open water with a few distant icebergs to open water areas partly covered by large clusters of ice floes. Analysis of these measurements reveals much the same variance in the ambient noise levels as found during previous measurements and the recorded noise was found to be composed of transient sound bursts of variable strength, superimposed on a continuously broad band noise as found during the Scoresbysund measurements. Upper and lower limiting envelopes of the measured noise spectra are given in Figure 4.5 together with the Scoresbysund data and the data obtained by Leggat for the central Baffin Bay.

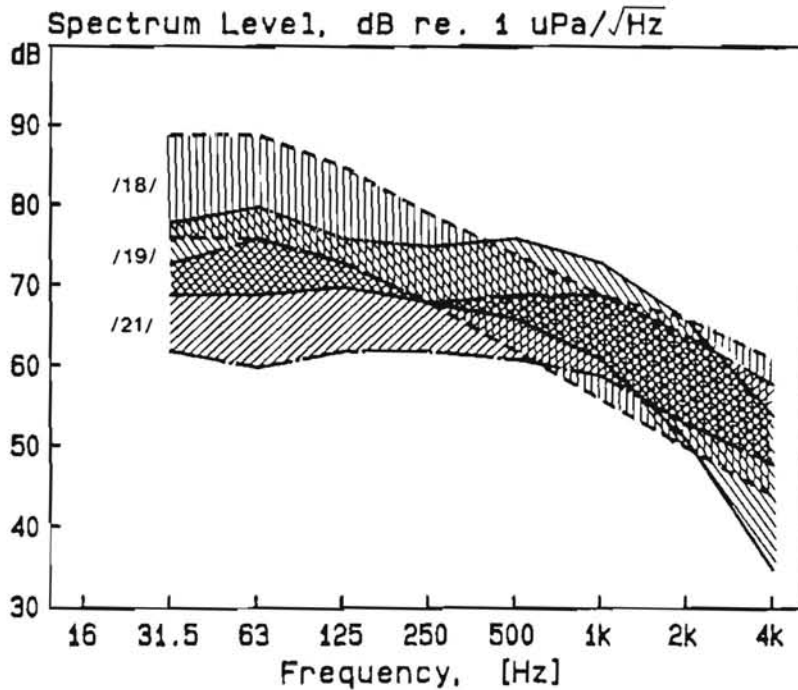


Figure 4.5.

Envelopes of ambient noise spectra measured off Thule, Thiele /21/ during summer conditions as compared with the data obtained off Scoresbysund, Thiele /19/ and in Baffin Bay, Leggat et al. /18/. Noise levels in dB re. $1 \mu\text{Pa}/\text{Hz}^{1/2}$.

Comparison of the limiting noise envelopes given in Figure 4.5 reveals that the ambient noise levels obtained off Thule are approximately of the same magnitude as data obtained off Scoresbysund and in the Baffin Bay for frequencies above 1000 Hz. At low frequencies the Thule measurements tend to be 8 dB lower than the Scoresbysund data and up to 15 dB lower than the Baffin Bay data. A comparison between the Kap York data and the Thule data as done in Figure 4.6, clearly demonstrates the salient features of arctic ambient noise spectra obtained during winter and summer conditions.

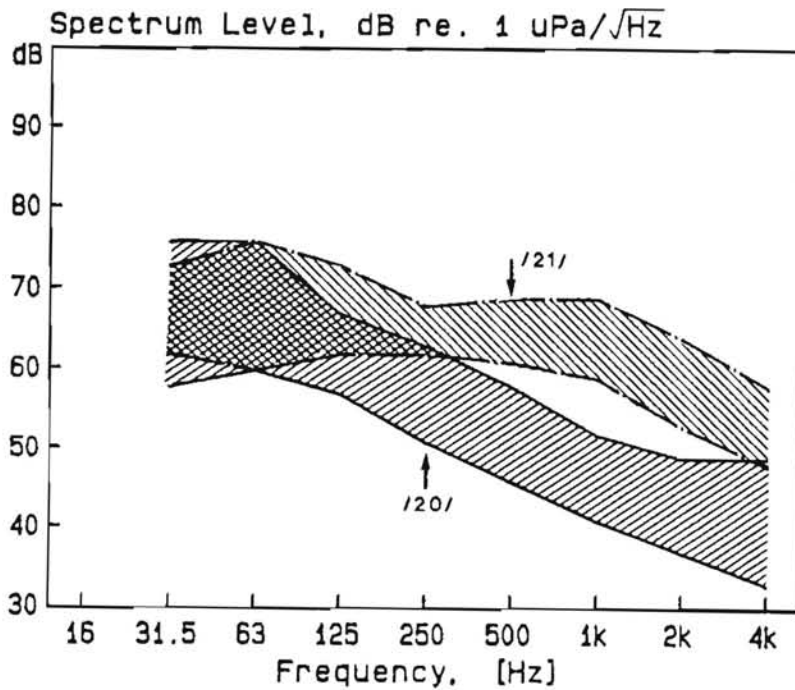


Figure 4.6.

Envelopes of ambient noise spectra measured off Thule, Thiele /21/ during summer conditions as compared with noise envelopes obtained off Kap York, Thiele /20/ during winter conditions. Noise levels in dB re. 1 $\mu\text{Pa}/\text{Hz}^{1/2}$.

A study of Figure 4.6 reveals that summer and winter ambient noise does not differ much at frequencies below 125 hz. At high frequencies the levels measured during summer conditions are up to 20 dB higher than the levels obtained during winter conditions. A possible explanation of the similarities and differences observed is that the low frequency part of the ambient noise spectrum is due to cracking and breaking up of the ice which occur during summer as well as during winter. The high frequency part of the summer spectrum is probably dominated by noise due to bubbles released by the melting ice, an effect which is absent during winter conditions.

All Arctic ambient noise data presented above were obtained as mean levels of short term measurements made within a few days or a few weeks. The pronounced non-gaussian properties of the ambi-



ent noise reported by the various researchers make it virtually impossible to establish a complete statistical description of the noise process. The measurement techniques employed would, in most ocean areas, yield reliable measures of the statistical properties of the ambient noise, this is however, not necessarily true for the Arctic waters in question.

Under the highly variable noise conditions found in Arctic waters, long-term measurements would be required in order to quantify the probability of a certain ambient noise level being detected at a particular location. Despite the somewhat limited amount of noise statistics, typical average ambient noise spectra suitable for noise exposure modelling will be suggested. Although available data support the shape and level of the suggested ambient noise spectra, it is not likely that a specific excess of the typical ambient noise spectra can be given.

4.3 Suggested Ambient Noise Spectra for Noise Exposure Modelling

In order to determine the typical ambient noise spectra suitable for noise exposure modelling in Arctic waters, the available upper and lower ambient noise envelopes were plotted in two separate figures according to season. Direct comparison of the ambient noise envelopes combined with knowledge about the spectral behaviour of the noise sources involved, allows an estimate to be made of the characteristic ambient noise spectra which are likely to be encountered during summer and winter conditions, respectively. It should be noted that the levels presented are the mean values averaged over a period of time.

Figure 4.7 which shows summer conditions, compare ambient noise data obtained by Leggat et al /18/, Milne and Ganton /15/, Diachok and Winokur /17/ and Thiele /19/, /21/. Additional ambient noise data obtained in the Baffin Bay by Thiele /9/ in connection with the "John A MacDonald" study are also given and they support the trends outlined by the ambient noise measurements mentioned in the previous section.

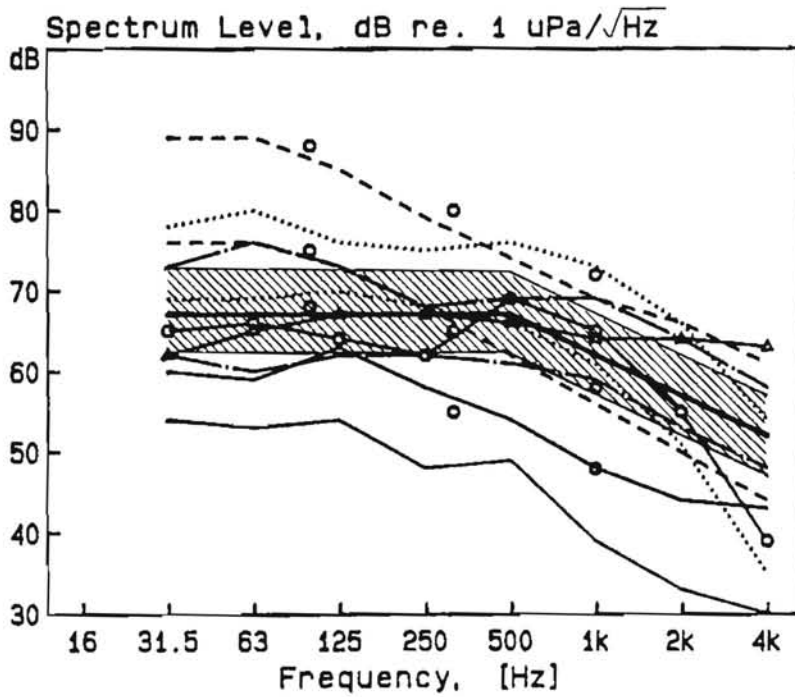


Figure 4.7.
Suggested average ambient noise spectrum for summer conditions, superimposed on ambient noise data given by various authors. Noise levels in dB re. 1 $\mu\text{Pa}/\text{Hz}^{1/2}$.

- | | | | | | |
|-----|--------|-------|--------|-----|--------|
| --- | : /18/ | | : /19/ | —.— | : /21/ |
| — | : /15/ | —○— | : /9/ | —△— | : /9/ |
| ○ | : /17/ | | | | |

A study of Figure 4.7 reveals the pronounced variability of ambient noise in arctic waters, the difference between the highest and the lowest noise levels being as much as 35 dB. Apart from the extremes, most ambient noise envelopes tend to group around a mean level given by the heavy broken line in Figure 4.7. This mean level is suggested as the ambient noise spectrum characteristic for summer conditions. The shaded band extending 5 dB above and below the suggested ambient noise level indicates the estimated order of magnitude of variations to be expected when comparing space and time averages of measured ambient noise data with the characteristic ambient noise spectrum suggested above and given in tabulated form in Table 4.1 below.



f	31.5	63	125	250	500	1K	2K	4K	Hz

L _a	67	67	67	67	67	62	57	52	dB

Table 4.1.

Suggested characteristic average ambient noise spectrum for summer conditions given at 1/1-octave standard frequencies. Noise levels in dB re. $1 \mu\text{Pa}/\text{Hz}^{1/2}$.

Figure 4.8 compare ambient noise measurements obtained during winter conditions by Milne and Ganton /15/ and by Thiele /20/. Additional ambient noise data obtained by Thiele /9/ under a cover of fast ice in Lancaster Sound are included and they follow the trends given by the ambient noise measurements reported in references Milne and Ganton /15/ and Thiele /20/.

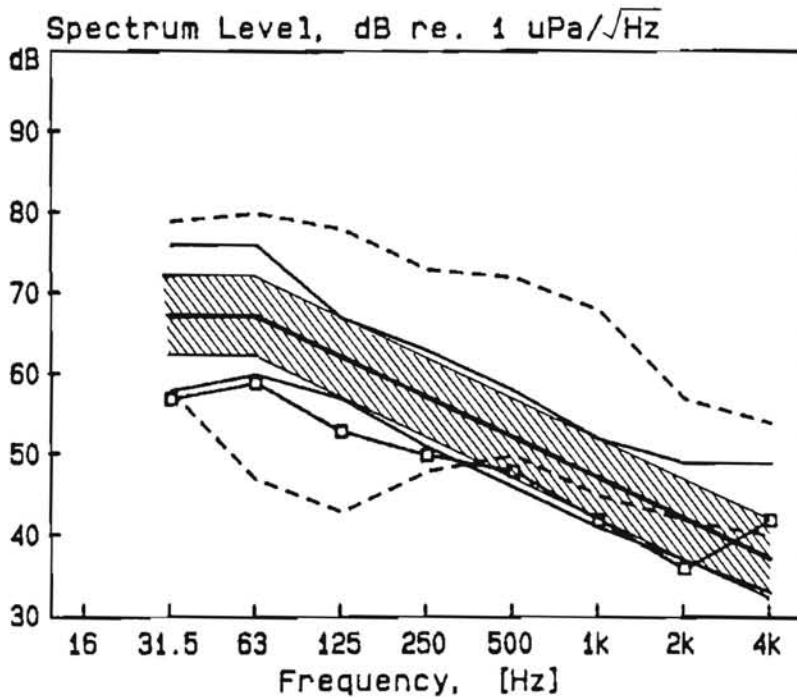


Figure 4.8.

Suggested average ambient noise spectrum for winter conditions superimposed on ambient noise data given by various authors. Noise levels in dB re. $1 \mu\text{Pa}/\text{Hz}^{1/2}$.

----- : /15/ ——— : /20/ —□— : /9/



As seen from Figure 4.9 the ambient noise levels during winter conditions may vary as much as ambient noise levels measured during summer conditions. With the exception of the highest ambient noise spectrum most of the ambient noise data tend to group around a mean level indicated by the heavy broken line in Figure 4.9. This mean level is suggested as the ambient noise spectrum characteristic for winter conditions. The shaded band extending 5 dB above and below the suggested ambient noise level indicates the estimated order of magnitude of variations when an average of measured ambient noise data are compared with the characteristic ambient noise spectrum suggested above and given in tabulated form in Table 4.2 below.

f	31.5	63	125	250	500	1K	2K	4K	Hz

L _a	67	67	62	57	52	47	42	37	dB

Table 4.2.

Suggested characteristic average ambient noise spectrum for winter conditions given at 1/1-octave standard frequencies. Noise levels in dB re. $1 \mu\text{Pa}/\text{Hz}^{1/2}$.

5. NOISE EXPOSURE MODEL

As described in Section 1, marine mammals in Arctic waters will be exposed to noise levels higher than the ambient noise because of shipping. The assessment of the impact of such underwater noise depends on,

- the amplitude of the ship generated noise relative to the ambient noise,
- the duration of time in which the noise level exceeds the ambient noise, and
- the extent of the area in which the ambient noise level is exceeded.



The present noise exposure model has been developed with the purpose of illustrating these effects in an easily interpretative way which can be useful in connection with future evaluations of shipping projects. The model has been developed for use in the Arctic but is not limited to this area and may consequently be used wherever shipping noise is expected to be a problem.

5.1 General Programme Description

As described in Section 1.3, the underwater noise exposure is basically modelled by the passive sonar equation which reads:

$$L_d = L_s - TL - L_a$$

where

L_d is the detection level above ambient

L_s is the source strength level

TL is the transmission loss and

L_a is the ambient noise level

Based on this model a computer programme has been developed which illustrates the variations of the detection level over a certain area and the variation with time at a certain point. The basic structure of the computer programme is illustrated in Figure 5.1.

Basically the programme can calculate the noise exposure in two different ways, illustrated by the right and left side of Figure 5.1. The calculation of the variation of the detection level spectra with time is illustrated by the right side of the figure. In this case the noise exposure has been calculated for a fixed point called the "observation point". For this point, the detection level spectra have been calculated for the noise generated by the ship at a number of points on the sailing route spaced with a constant time interval.

The left side of Figure 5.1 illustrates the calculation of the extent of area which is being exposed to noise higher than the ambient noise level. This calculation can be carried out for the

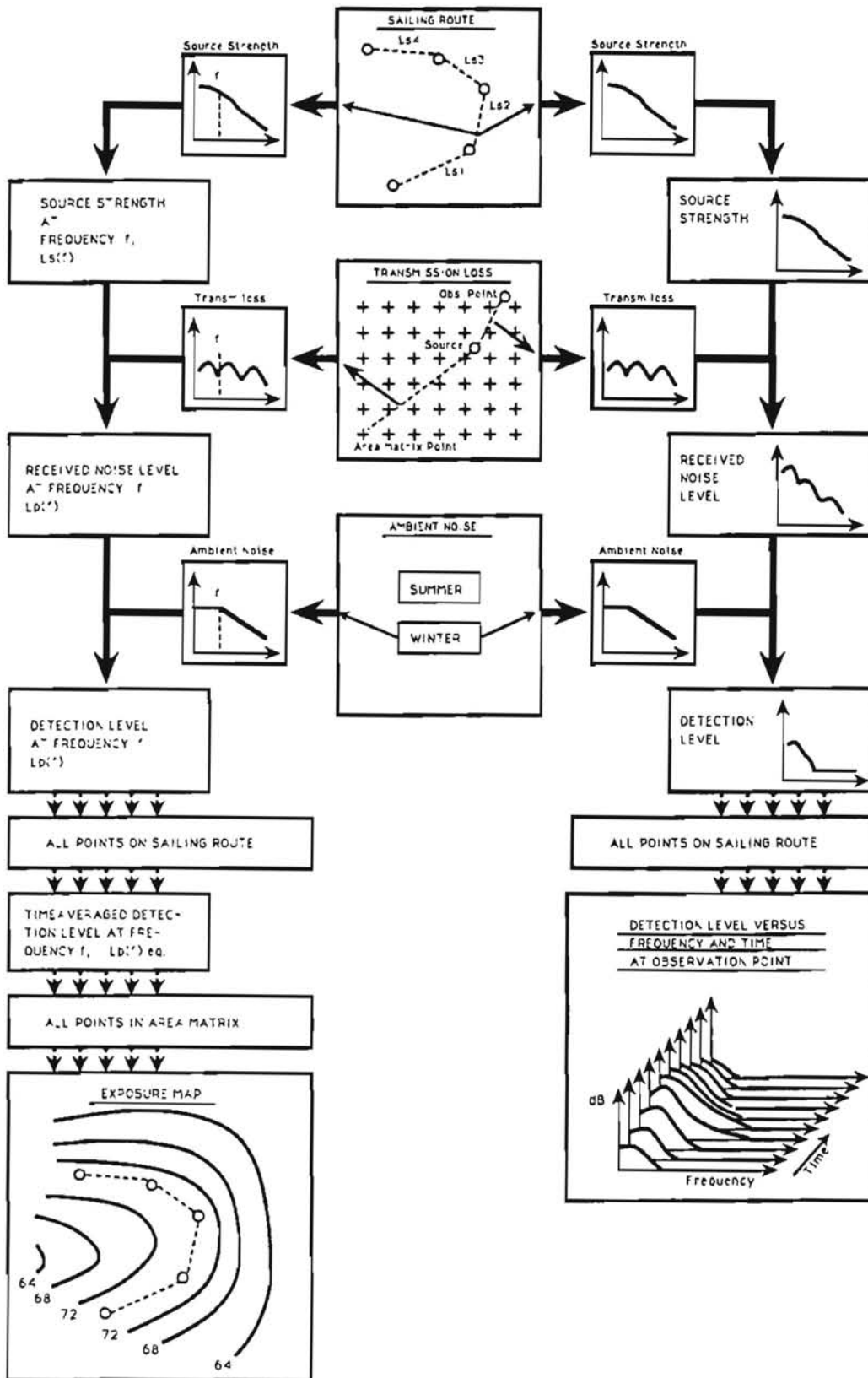


Figure 5.1. Programme structure for the noise exposure model.



noise at single 1/3-octave frequency band. The area being investigated has been divided into a 87 x 87 point matrix and for each of these points the sound pressure level has been calculated for noise generated at all points on the sailing route.

For each matrix point the equivalent sound pressure level has been calculated from the sum of the received levels divided by the total number of time steps along the route. Based on these results a contour plot has been drawn. Negative detection levels are not drawn which means that the last contour curve represents the distance from the route where the received equivalent ship noise is equal to the ambient noise.

The scaling of the output plot is fitted to the standard "Mercator projection" which normally is applied for sea charts. It is therefore possible to apply the calculated exposure map directly with the sea charts in order to illustrate the noise exposure. The detailed input and output parameters are discussed in Sections 5.2 and 5.3. Realistic examples of the application of the noise exposure programme are given in Section 6.

5.2 Input Parameters

The input for the underwater noise exposure computer programme is performed via menus. The opening menu of the programme is shown in Figure 5.2.

The various input parameters for the underwater noise exposure programme are illustrated in Figure 5.2. These are the source data, background noise, transmission loss and routes.

The source data input is illustrated in Figure 5.3. Up to twenty different source numbers can be defined by the noise source level in 1/3-octave frequency bands with centre frequencies from 31.5 Hz to 4000 Hz and the speed of the ship. The source levels can be measured data or predicted data derived from the theory described in Section 2.



```
----- GET NO. ----- [ CALCULATE JOB ] [ COPY JOB ] [ EXIT ]
                        UNDERWATER NOISE EXPOSURE DATAFILE: uwmac.d
-----
NO  CATALOGS
-2  SOURCE DATA CATALOG
-1  BACKGROUND NOISE CATALOG
 0  TRANSMISSION LOSS CATALOG
-----
NO.  ROUTES                                DATE  INIT
 1  John A. MacDonald                      880623  a1
 2  Test                                    900110  11
 3  Test No.2                              310588  bv
 4  John A. McDonald (const. speed)        880623  a1
 5  Centre Route Baffin Bay                900212  11
 6  Seismic ship short distance            900216  11
 7  Winter Route Along W.Coast             881031  11
 8  Seismic ship curved route              900214  11
 9  West Coast Route.                      900125  11

SELECT KEYFUNCTION or
Press RETURN to continue
```

Figure 5.2.

Example of opening menu for noise exposure programme.

The background noise input is also illustrated in Figure 5.3. A maximum of twenty different ambient noise spectra can be defined in 1/3-octaves from 31.5 Hz to 4000 Hz.

Finally, the input for the sound transmission loss is illustrated in the lower part of Figure 5.3. The sound transmission loss in 1/3-octaves can be given for up to twenty different distances. The input can be measured data or calculated data derived from the prediction models described in Section 3. The transmission loss at other distances than those given in the input data are found by logarithmic interpolation. If no transmission loss data are given or the distance is larger than the maximum distance stated, then the transmission loss is calculated in the programme using the empirical model described in Section 3.4. The attenuation coefficients applied for this model depend on the choice between ice covered or open water condition, selected in the route input, and the water depth and sea state values given for each route point.



GET NUMBER		DELETE SOURCE		PRINT SOURCE		MAIN MENU	
SOURCE CATALOG (Max. 20)							
No.	SOURCE	TEXT	SPEED				
1	Source 1	(Openwater)	10.0				
2	Source 2		8.0				
3	Source 3		8.0				
4	Source 4	(Ice)	8.0				
5	Source 5	(Heavy ice)	4.0				
6	test	200 dB all	10.0				

Text = Source 1 (Openwater)
 Speed = 10.0 knot
 Source depth = 8.0 m

1/3-OCTAVE											
31.5	40	50	63	80	100	125	160	200	250	315	Hz
159.2	159.2	159.2	159.2	159.2	159.2	157.2	155.2	155.2	151.2	149.2	dB
400	500	630	800	1000	1250	1600	2000	2500	3150	4000	Hz
147.2	145.2	142.2	141.2	139.2	137.2	135.2	133.2	131.2	129.2	127.2	dB

GET NUMBER		DELETE BACK		PRINT BACK		MAIN MENU	
BACKGROUND NOISE CATALOG (Max. 20)							
No.	BACK	NOISE	TEXT				
1	Arctic	(Summer)					
2	Arctic	(winter)					
3	test	50 dB all					

Text = Arctic (summer)

1/3-OCTAVE											
31.5	40	50	63	80	100	125	160	200	250	315	Hz
67.0	67.0	67.0	67.0	67.0	67.0	67.0	67.0	67.0	67.0	67.0	dB
400	500	630	800	1000	1250	1600	2000	2500	3150	4000	Hz
67.0	67.0	65.0	63.0	62.0	60.0	58.0	57.0	55.0	53.0	52.0	dB

GET NUMBER		DELETE TRANS		PRINT TRANS		MAIN MENU	
TRANSMISSION LOSS CATALOG (Max. 20)							
No.	TRANS	LOSS	TEXT				
1	Eaffin Eay	(Open w.)	675.0	m			
2	Eaffin Eay	(Open w.)	1700.0	m			
3	Eaffin Eay	(Open w.)	7770.0	m			
4	Eaffin Eay	(Open w.)	17800.0	m			
5	Eaffin Eay	(Open w.)	35000.0	m			

Text = Eaffin Eay (Open w.)
 Distance = 675.0 m

1/3-OCTAVE											
31.5	40	50	63	80	100	125	160	200	250	315	Hz
55.0	54.0	55.0	54.0	52.0	55.0	54.0	54.0	55.0	57.0	58.0	dB
400	500	630	800	1000	1250	1600	2000	2500	3150	4000	Hz
59.0	55.0	53.0	55.0	56.0	55.0	55.0	53.0	54.0	57.0	58.0	dB

Figure 5.3.
 Example of input parameters for source strength, back-ground noise and sound transmission loss.



SET NO.	DELETE NO.	FFINT ROUTE	MAIN MENU			
ROUTE: 9	POSITION NO.	LAT.	LONG.	BACK.	PROFILE TIME	
-1	MAIN DATA	69: 0: 0	-54: 0: 0	2	0 2.0	
	POSITION NO. (1-20)	LAT.	LONG.	SOURCE	DEPTH	SEA
1		58: 0: 0	-58: 0: 0	1	1000	0
2		60: 0: 0	-58: 0: 0	1	500	0
3		70: 0: 0	-58: 0: 0	2	300	0
4		74: 0: 0	-60: 0: 0	2	500	0
5		75:30: 0	-65: 0: 0	4	400	0
6		75:30: 0	-72: 0: 0	1	400	0
7		74: 0: 0	-80: 0: 0	3	500	0
8		74: 0: 0	-85: 0: 0	3	500	0

Figure 5.4.
Example of input data for sailing route definition.

The last input data are the definition of the route and the observation point as illustrated in Figure 5.4. The following input data should be given:

- Position of observation point. Given in latitude and longitude (N: +, S: -, E: +, W: -).
- Background noise in the area of the route. Given as a number in the "Background noise catalogue".
- Sound speed profile. Option to be selected is summer (1) or winter (0) condition. This input is used for the calculation of the sound transmission loss which is performed when no transmission data are specified.
- Time interval. The calculation is performed for a number of points placed stepwise along the route determined by this time interval and the speed of the ship.
- Sailing route. The route is defined by up to 20 points by their latitude and longitude. The source strength is given for each point by a number in the "source catalogue". This



source strength and the corresponding speed of the ship is applied for all locations along the route until a new route point is reached. The programme applies "great circle" distances when calculating the route and the transmission loss.

- The water depth and sea state. These parameters are given for each point on the route. The data are used for the calculation of the sound transmission loss when no transmission loss data are given.

5.3 Output

When the input data have been defined, the calculations can be started from the main menu by selecting a route number. In order to start up the calculation the following must be entered:

- Area for exposure map. Given as maximum and minimum latitude and longitude.
- Frequency. Centre frequency of the 1/3-octave frequency band to be used for exposure map or "0" for linear level.
- Contour line interval and min/max level.

The programme starts to calculate the equivalent sound pressure level for each of the 87 x 87 matrix points and the frequency spectra of the detection level at the observation point for the time steps corresponding to the points on the sailing route spaced with the specified time interval.

The presentation of the results can be selected from the output menu as a contour plot (exposure plot) or "waterfall" plots of the receiver and detection levels.

Examples of the output data are illustrated in Figures 5.5 and 5.6.

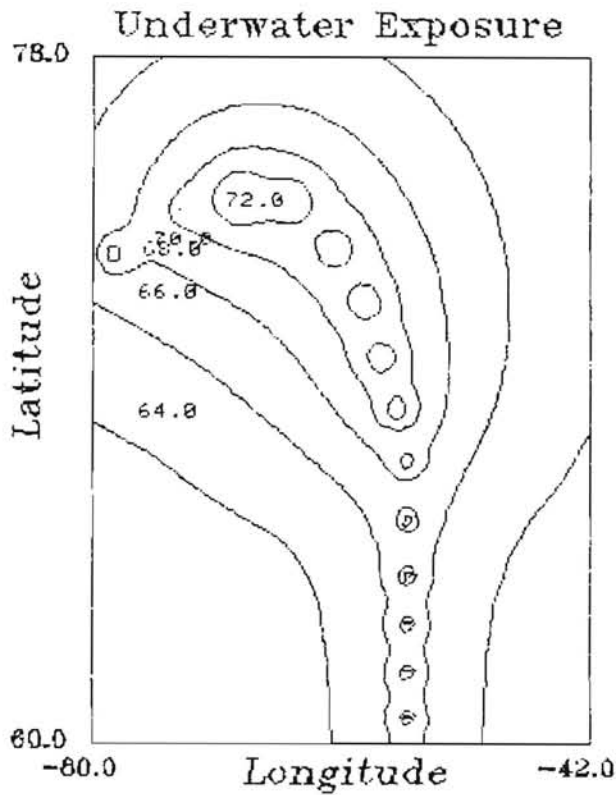


Figure 5.5.

Example of the output from the contour plot showing the sound pressure level contours at a single 1/3-octave frequency band.

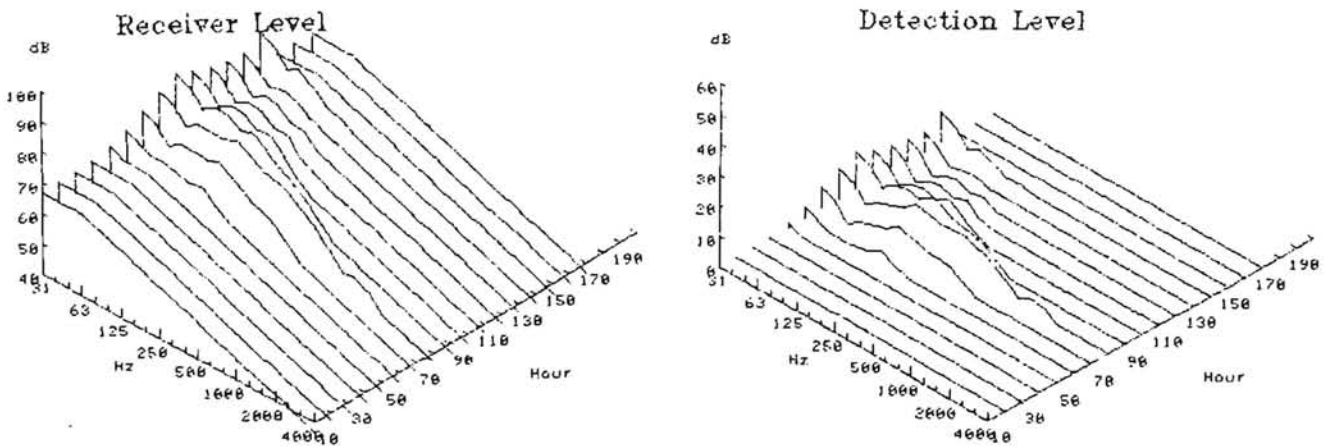


Figure 5.6.

Example of the output from the "waterfall" plots showing the variation in receiver level and detection level with time.



The contour plot illustrated in Figure 5.5 has been plotted in "Mercator projection" as this projection normally is used for sea charts. It is therefore possible directly to transfer the contour lines from the exposure plot to a sea chart applying a simple scale factor. The "dots" seen in Figure 5.5 illustrate the effect of the steps along the sailing route. When a short time interval is selected, the curves will be more smooth but the calculation time will increase.

Figure 5.7 illustrates a contour plot applied to the sea chart from the area.

Underwater Exposure

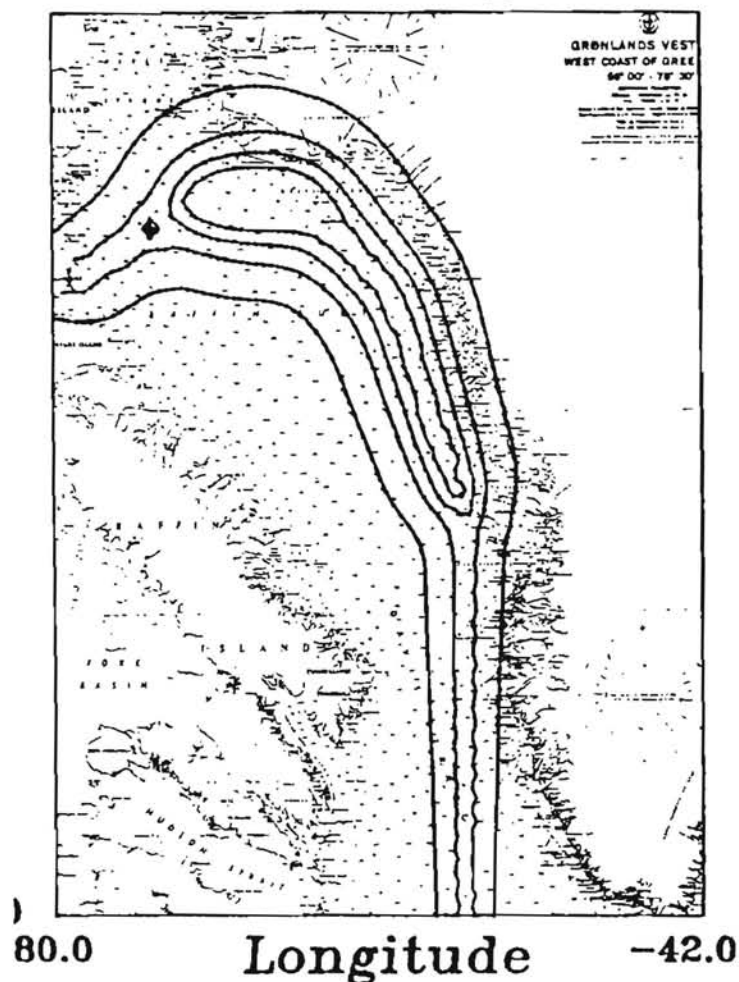


Figure 5.7.
Example of contour plot applied to the sea chart.



6. EXAMPLES OF UNDERWATER NOISE EXPOSURE FROM SHIPPING

The present examples are given in order to illustrate the use of the underwater noise exposure programme for realistic combinations of ship, route and area. The Baffin Bay and Davis Strait have been selected for the examples as these are located in an area where ship traffic might be increased in the future. The icebreaker John A. McDonald is selected as a realistic example of a ship to pass through the area along two different routes in a summer and a winter condition. Examples are also given which simulate an APP-tanker sailing in the centre of Baffin Bay and a vessel with the size of a large fishing trawler or a seismic ship sailing along the west coast of Greenland off Disko Island.

6.1 Input Data

The area selected for the exposure calculations is illustrated in Figures 6.1 and 6.2. The area covered an extent from latitude 60°N to 78°N and from longitude 42°W to 80°W .

Two different routes have been selected for the noise exposure examples as illustrated in Figures 6.1 and 6.2. The central route passes through the middle of the Davis Strait and Baffin Bay and continues out through Lancaster Sound as illustrated in Figure 6.1.

The solid line in Figures 6.1 and 6.2 represents the route defined by the route points marked with numbers. The starting point and end point are located outside the area used for the exposure map in order to make the contour lines more smooth.

The west coast route illustrated in Figure 6.2 passes close by the West Greenland coast up to Kap York and then continues out through Lancaster Sound. This route is generally used during

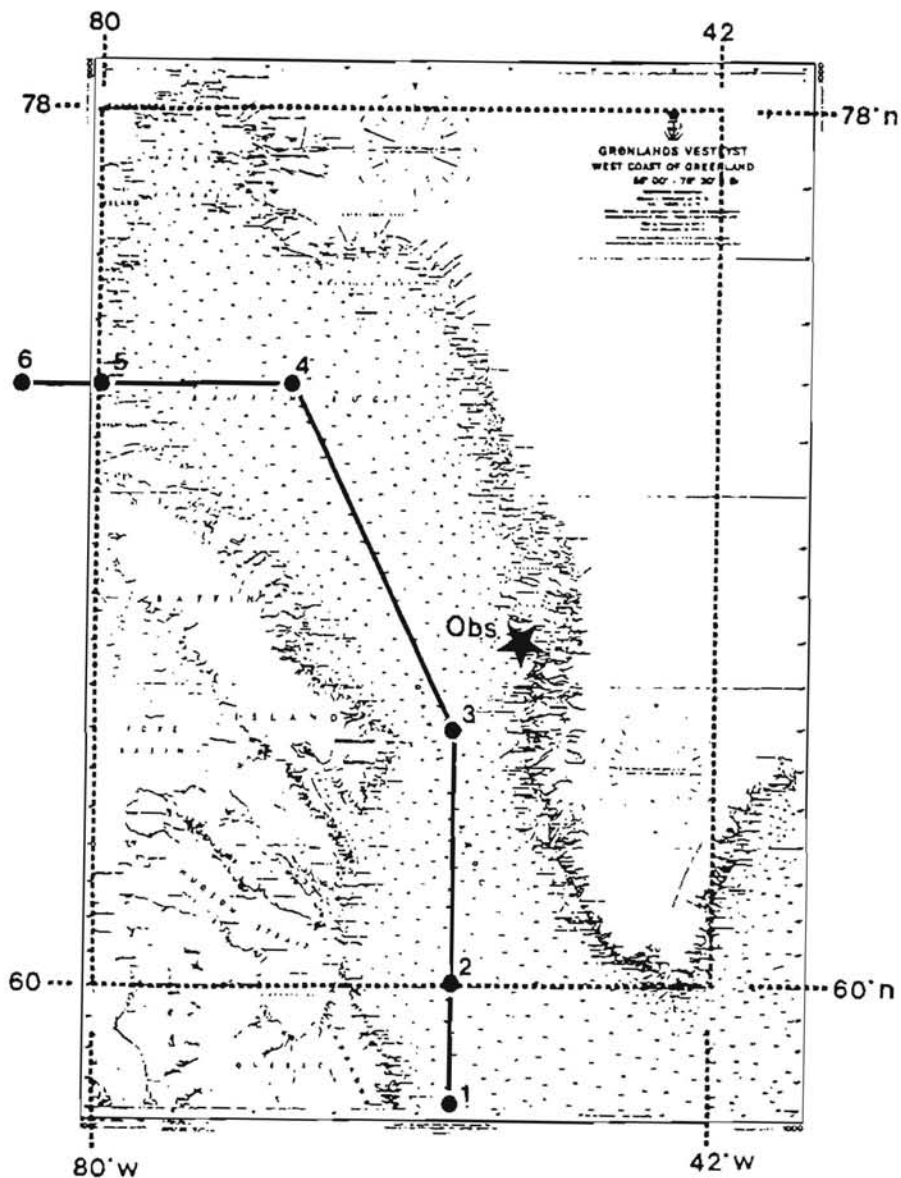


Figure 6.1.

Area used for exposure modelling of the central route and location of the observation point south of Disko Island.

winter time due to the lower ice concentration along the West Greenland coast compared with the thicker ice in the centre and western Baffin Bay.

The observation points selected are south of Disko (69°N , 54°W) and off Kap York (76°N , 66°W).

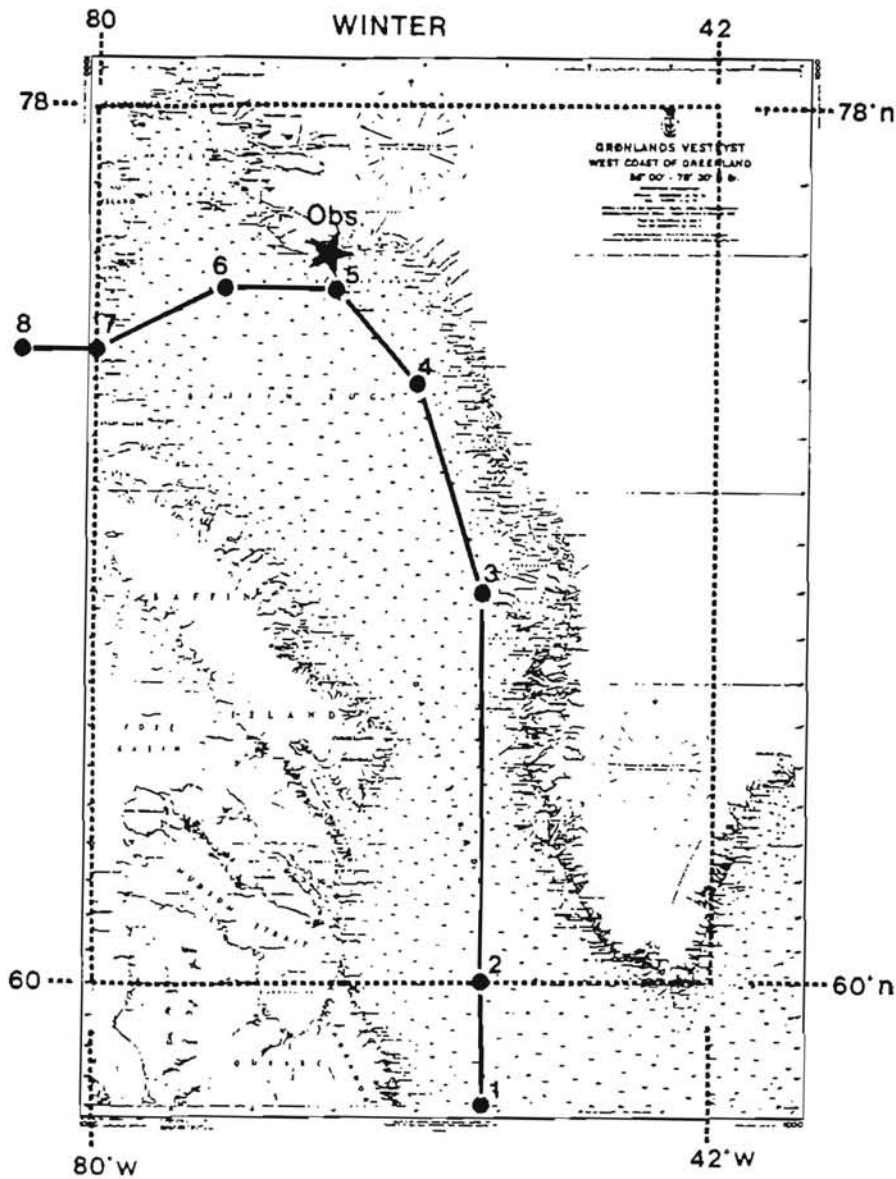


Figure 6.2.
Area used for the west coast route and location of the
observation point at Kap York.

During the summer condition the load condition of the icebreaker and the seismic ship is assumed to be constant while load variations are assumed during the winter condition, simulating different ice conditions. The various source strengths applied appear from Table 6.1. The source strength levels have been calculated from the prediction model derived by N. Brown as described in Section 2.



UNDERWATER EXCELTE SOURCE DATA

PAGE: 1

SOURCE NO. 1 : Source 1 (Openwater) SPEED : 10.0 Knot SOURCE DEPTH : 8 M											
FREQ. (Hz)	31.5	40	50	63	80	100	125	160	200	250	315
SOURCE(dB)	159.2	159.2	159.2	159.2	159.2	159.2	157.2	155.2	153.2	151.2	149.2
FREQ. (Hz)	400	500	630	800	1000	1250	1600	2000	2500	3150	4000
SOURCE(dB)	147.2	145.2	143.2	141.2	139.2	137.2	135.2	133.2	131.2	129.2	127.2
SOURCE NO. 2 : Source 2 (Packice) SPEED : 3.0 Knot SOURCE DEPTH : 8 M											
FREQ. (Hz)	31.5	40	50	63	80	100	125	160	200	250	315
SOURCE(dB)	156.1	156.1	156.1	156.1	156.1	154.1	152.1	150.1	150.1	156.1	154.1
FREQ. (Hz)	400	500	630	800	1000	1250	1600	2000	2500	3150	4000
SOURCE(dB)	152.1	150.1	148.1	146.1	144.1	142.1	140.1	138.1	136.1	134.1	132.1
SOURCE NO. 3 : Source 3 (Open, low) SPEED : 8.0 Knot SOURCE DEPTH : 8 M											
FREQ. (Hz)	31.5	40	50	63	80	100	125	160	200	250	315
SOURCE(dB)	150.0	150.0	150.0	150.0	150.0	150.0	150.0	148.0	146.0	144.0	142.0
FREQ. (Hz)	400	500	630	800	1000	1250	1600	2000	2500	3150	4000
SOURCE(dB)	140.0	138.0	136.0	134.0	132.0	130.0	128.0	126.0	124.0	122.0	120.0
SOURCE NO. 4 : Source 4 (Heavy ice) SPEED : 3.0 Knot SOURCE DEPTH : 8 M											
FREQ. (Hz)	31.5	40	50	63	80	100	125	160	200	250	315
SOURCE(dB)	170.3	170.3	170.3	170.3	168.3	166.3	164.3	162.3	160.3	158.3	156.3
FREQ. (Hz)	400	500	630	800	1000	1250	1600	2000	2500	3150	4000
SOURCE(dB)	154.3	152.3	150.3	148.3	146.3	144.3	142.3	140.3	138.3	136.3	134.3
SOURCE NO. 5 : Source 5 APP tanker SPEED : 12.0 Knot SOURCE DEPTH : 8 M											
FREQ. (Hz)	31.5	40	50	63	80	100	125	160	200	250	315
SOURCE(dB)	182.0	180.0	178.0	176.0	174.0	172.0	170.0	168.0	166.0	164.0	162.0
FREQ. (Hz)	400	500	630	800	1000	1250	1600	2000	2500	3150	4000
SOURCE(dB)	160.0	158.0	156.0	154.0	152.0	150.0	148.0	146.0	144.0	142.0	140.0
SOURCE NO. 6 : Seismic ship SPEED : 4.0 Knot SOURCE DEPTH : 2 M											
FREQ. (Hz)	31.5	40	50	63	80	100	125	160	200	250	315
SOURCE(dB)	145.0	145.0	145.0	145.0	145.0	145.0	143.0	141.0	139.0	137.0	135.0
FREQ. (Hz)	400	500	630	800	1000	1250	1600	2000	2500	3150	4000
SOURCE(dB)	133.0	131.0	129.0	127.0	125.0	123.0	121.0	119.0	117.0	115.0	113.0

Table 6.1.

Print out of the source strength levels, dB re 1 $\mu\text{Pa}/\sqrt{\text{Hz}}$, applied for the noise exposure calculations.



The sound transmission loss applied for the calculations is found from the measured data from Baffin Bay obtained during the investigation performed from the icebreaker John A. McDonald as described in Section 3.

The transmission loss is given for a receiver depth of 50 metres and for five distances extending to a distance of 35 km. The transmission losses at the centre frequencies of the 1/3-octave frequency bands from 31.5 Hz to 4000 Hz are given in Table 6.3.

It should be noted that at distances larger than 35 km, the transmission loss is calculated from the prediction model as described in Section 3.5. Compared with the area used for the exposure calculations, 35 km are only a short distance and consequently the prediction model is used for major parts of the area.

The ambient noise level in the area of investigation is selected according to the "summer" and "winter" spectra described in Tables 4.1 and 4.2. The levels are shown in Table 6.2.

UNDERWATER EXPOSURE BACKGROUND NOISE DATA

PAGE: 1

BACKGROUND NOISE NO. 1 : Artic (Summer)											

FREQ. (Hz)	31.5	40	50	63	80	100	125	160	200	250	315
BACK. (dB)	67.5	67.6	67.0	67.0	67.0	67.0	67.0	67.0	67.0	67.0	67.0

FREQ. (Hz)	400	500	630	800	1000	1250	1600	2000	2500	3150	4000
BACK. (dB)	67.0	67.0	65.3	63.7	62.0	60.3	58.7	57.0	55.3	52.7	52.0

BACKGROUND NOISE NO. 2 : Artic (Winter)											

FREQ. (Hz)	31.5	40	50	63	80	100	125	160	200	250	315
BACK. (dB)	67.0	67.0	67.0	67.0	65.3	63.7	62.0	60.3	58.7	57.0	55.3

FREQ. (Hz)	400	500	630	800	1000	1250	1600	2000	2500	3150	4000
BACK. (dB)	53.7	52.0	50.3	48.7	47.0	45.3	43.7	42.0	40.3	38.7	37.0

Table 6.2.

Print out of the average ambient noise levels, dB re 1 $\mu\text{Pa}/\sqrt{\text{Hz}}$, applied for the noise exposure calculations.



UNDERWATER EXPOSURE TRANSMISSION LOSS DATA

PAGE: 1

TRANSMISSION LOSS NO. 1 : Baffin Bay (Open W.)												
DISTANCE FROM SOURCE 675.0 m												
FREQ. (Hz)	31.5	40	50	63	80	100	125	160	200	250	315	
TRANS. (dB)	53.0	54.0	59.0	54.0	52.0	55.0	54.0	54.0	55.0	57.0	58.0	
FREQ. (Hz)	400	500	630	800	1000	1250	1600	2000	2500	3150	4000	
TRANS. (dB)	59.0	55.0	53.0	55.0	56.0	55.0	55.0	53.0	54.0	57.0	58.0	
TRANSMISSION LOSS NO. 2 : Baffin Bay (Open W.)												
DISTANCE FROM SOURCE 1700.0 m												
FREQ. (Hz)	31.5	40	50	63	80	100	125	160	200	250	315	
TRANS. (dB)	67.0	66.0	64.0	66.0	59.0	58.0	58.0	57.0	54.0	54.0	53.0	
FREQ. (Hz)	400	500	630	800	1000	1250	1600	2000	2500	3150	4000	
TRANS. (dB)	57.0	62.0	61.0	60.0	58.0	57.0	59.0	62.0	58.0	63.0	60.0	
TRANSMISSION LOSS NO. 3 : Baffin Bay (Open W.)												
DISTANCE FROM SOURCE 7770.0 m												
FREQ. (Hz)	31.5	40	50	63	80	100	125	160	200	250	315	
TRANS. (dB)	72.0	74.0	78.0	77.0	78.0	79.0	75.0	71.0	70.0	69.0	68.0	
FREQ. (Hz)	400	500	630	800	1000	1250	1600	2000	2500	3150	4000	
TRANS. (dB)	68.0	70.0	74.0	75.0	70.0	70.0	75.0	72.0	76.0	76.0	77.0	
TRANSMISSION LOSS NO. 4 : Baffin Bay (Open W.)												
DISTANCE FROM SOURCE 17800.0 m												
FREQ. (Hz)	31.5	40	50	63	80	100	125	160	200	250	315	
TRANS. (dB)	81.0	77.0	84.0	75.0	74.0	78.0	76.0	73.0	75.0	72.0	71.0	
FREQ. (Hz)	400	500	630	800	1000	1250	1600	2000	2500	3150	4000	
TRANS. (dB)	71.0	74.0	75.0	78.0	77.0	79.0	78.0	78.0	81.0	77.0	80.0	
TRANSMISSION LOSS NO. 5 : Baffin Bay (Open W.)												
DISTANCE FROM SOURCE 35000.0 m												
FREQ. (Hz)	31.5	40	50	63	80	100	125	160	200	250	315	
TRANS. (dB)	78.0	80.0	85.0	82.0	82.0	82.0	78.0	78.0	78.0	77.0	76.0	
FREQ. (Hz)	400	500	630	800	1000	1250	1600	2000	2500	3150	4000	
TRANS. (dB)	77.0	78.0	80.0	82.0	76.0	77.0	85.0	78.0	82.0	88.0	89.0	

Table 6.3.

Print out of the sound transmission loss applied for the noise exposure calculations.



6.2 Results

The presentation of the following results has been selected to illustrate the use of the programme but is not intended to give the full and detailed results for each example.

The results obtained for the four examples are illustrated in Figures 6.3-6.6 and are presented as the exposure maps for the 1/3-octaves with centre frequencies 100 Hz and 1000 Hz, and the detection level versus time for the two observation points at Kap York and Disko.

Example 1

The first calculated example, illustrates the John A. MacDonald sailing along the central route shown in Figure 6.1. The source strength applied for this example is for all route points the "Open water 10 Knots" given as source No. 1 in Table 6.1. The ambient noise is selected to be "Arctic Summer" given as background noise No. 1 in Table 6.3. The results from the first example are given in Figure 6.3.

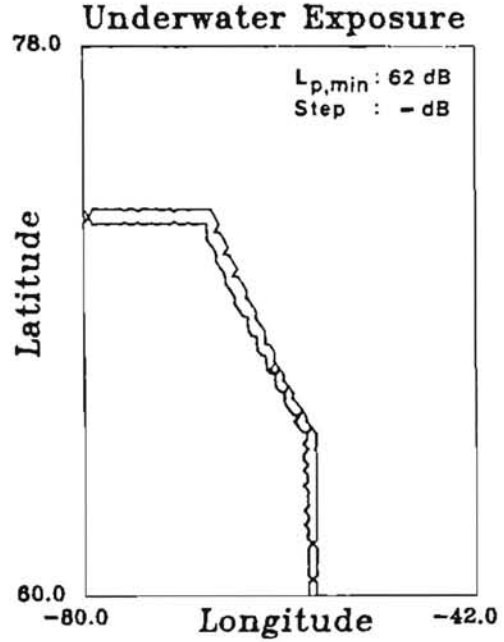
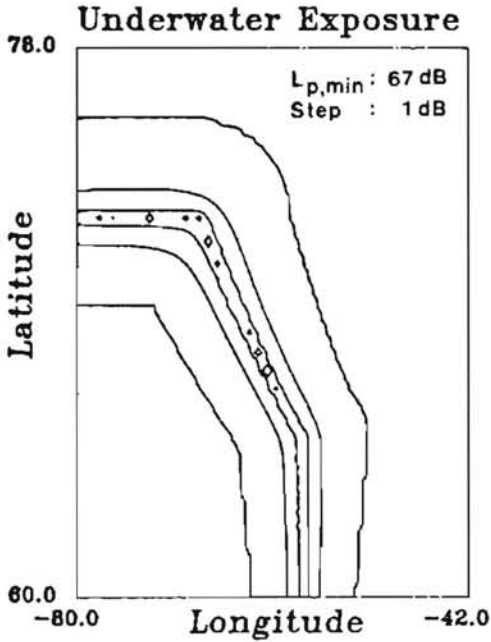
The two upper curves are the exposure contour plots for 100 Hz and 1000 Hz. From these curves it can be seen that the exposed area is much larger at 100 Hz than at 1000 Hz. The reason for this is that the source strength has decreased by 20 dB while the ambient noise level has only decreased by 5 dB when the frequency was increased from 100 Hz to 1000 Hz. This effect is especially strong during summer conditions when the ambient noise spectra are flat all up to 500 Hz. Also the transmission loss is increasing at higher frequencies. This means that the ship noise reaches the ambient noise level at a shorter distance from the route when the frequency is increased.

In this first example the source strength of the ship is kept constant and the contour lines are consequently located at constant distances from the route. In the contour plot the lines



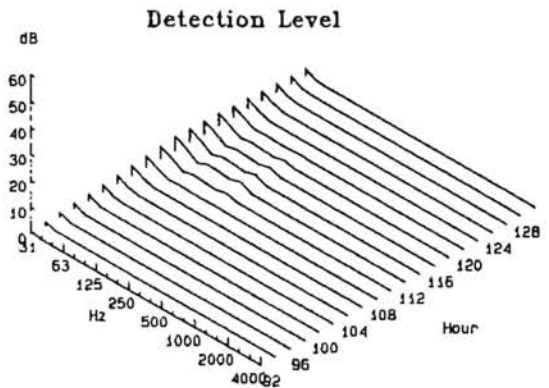
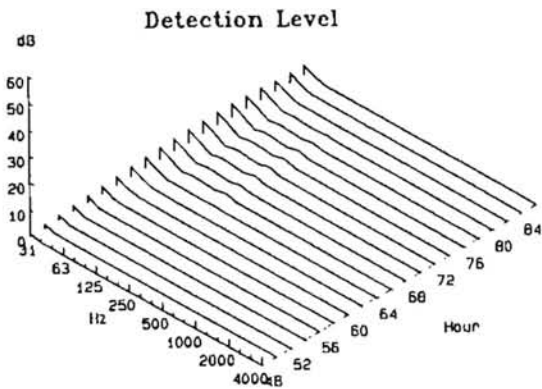
100 Hz:

1000 Hz:



Disko (69°N, 54°W):

Kap York (76°N, 66°W):



Input:

```

=====
ROUTE: 5  POSITION NO.    LAT.    LONG.    BACK.  PROFILE TIME
=====
-1  MAIN DATA  69: 0: 0  -54: 0: 0    1      0    2.0
=====
POSITION NO.(1-20)  LAT.    LONG.    SOURCE  DEPTH  SEP
-----
1                   58: 0: 0  -58: 0: 0    1     2000  1
2                   60: 0: 0  -58: 0: 0    1     3000  1
3                   67: 0: 0  -58: 0: 0    1       500  1
4                   74: 0: 0  -69: 0: 0    1     2000  1
5                   74: 0: 0  -60: 0: 0    1       500  1
6                   74: 0: 0  -65: 0: 0    1       500  1
=====

```

Figure 6.3.

Example 1. Icebreaker sailing along central route during summer conditions.



tend to spread a little when moving north. The reason for this is the Mercator projection which results in a "stretching" of the map due to a varying scale factor with the latitude.

The two lower curves show the variation of the detection level with time during passage of the observation points. The first observation point at Disko (left curve) is passed approximately 70 hours after the start of the ship at route point 1. At both observation points an influence can only be noted at low frequencies and with rather low amplitudes as both points are quite far from the sailing route.

Example 2

The second example illustrates the icebreaker sailing along the central route, the same as applied in the first example but this time during winter conditions. The source strength is therefore assumed to vary due to the changing ice conditions. The following source strengths have been selected along the route:

Point 1 - 2 :	Open water	Source strength No. 1.
Point 2 - 3 :	Pack ice	Source strength No. 2.
Point 3 - 4 :	Heavy ice	Source strength No. 4.
Point 4 - 5 :	Pack ice	Source strength No. 2.
Point 5 - 6 :	Open water	Source strength No. 1.

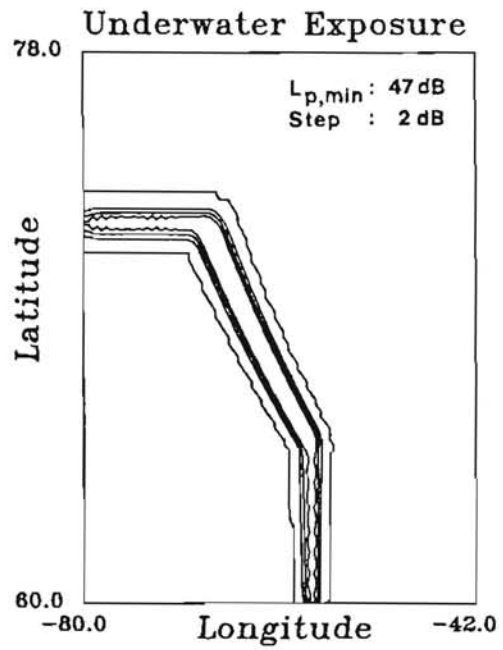
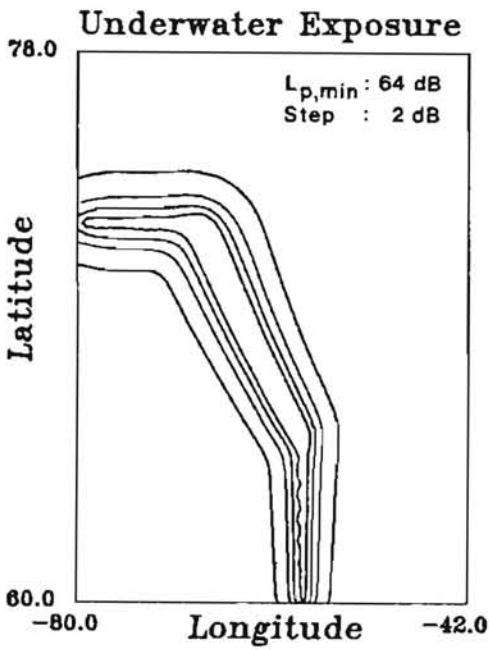
The ambient noise selected is the "Arctic Winter" given as background noise No. 2 in Table 6.3. The results are given in Figure 6.4.

As for the first example it can once more be seen that the exposed area is bigger for the low frequency (100 Hz) than for the high frequency (1000 Hz). However, the difference is less pronounced than for the summer condition as the winter ambient noise is lower and starts decreasing at a lower frequency than during summer condition. At 100 Hz the area of exposure is small compared with example 1 due to the increase in transmission loss caused by the ice-cover.



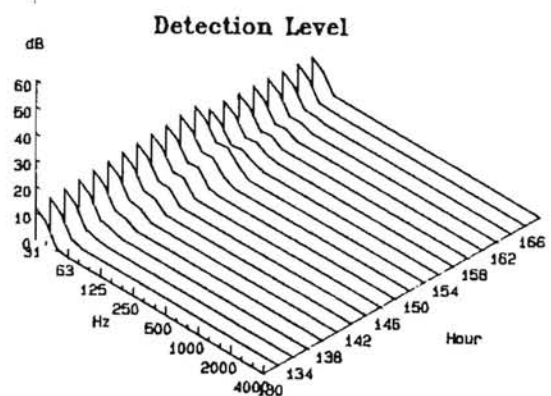
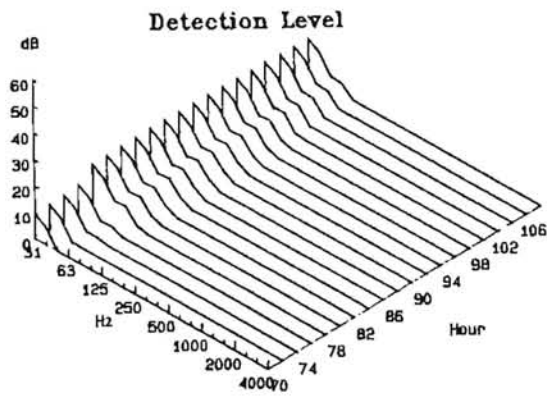
100 HZ:

1000 HZ:



Disko (69°N, 54°W):

Kap York (76°N, 66°W):



Input:

```

=====
ROUTE: 5  POSITION NO.    LAT.    LONG.    BACK.  PROFILE TIME
=====
-1  MAIN DATA  69: 0: 0  -54: 0: 0    2      1  2.0
=====
POSITION NO.(1-20)  LAT.    LONG.    SOURCE  DEPTH  SEA
-----
1      56: 0: 0  -58: 0: 0    1     2000  1
2      60: 0: 0  -58: 0: 0    2     3000  1
3      67: 0: 0  -58: 0: 0    4      800  1
4      74: 0: 0  -68: 0: 0    2     2000  1
5      74: 0: 0  -80: 0: 0    1      800  1
6      74: 0: 0  -85: 0: 0    1      800  1

```

Figure 6.4.
Example 2. Icebreaker sailing along central route during winter conditions.



The contour lines tend to spread out in the middle part of the route due to the increased source strength in this part.

For the observation point at Disko it can be seen that the detection level increases 78 hours after the start (source strength increases at route point 3) and that the level does not vary much during the passage. This is due to the low speed assumed for the ship sailing in the heavy ice condition occurring after route point 3. A similar step in the detection level can be seen for the Kap York observation point 154 hours after the start when the source strength is reduced after route point 4.

Example 3

This example illustrates the icebreaker sailing along the west coast route shown in Figure 6.2. Again winter conditions are assumed which result in different load conditions varying with the ice conditions. The following source strengths have been applied:

Point 1 - 2 :	Open water	Source strength No. 1.
Point 2 - 3 :	Open water	Source strength No. 1.
Point 3 - 4 :	Pack ice	Source strength No. 2.
Point 4 - 5 :	Pack ice	Source strength No. 2.
Point 5 - 6 :	Heavy ice	Source strength No. 4.
Point 6 - 7 :	Open water	Source strength No. 1.
Point 7 - 8 :	Open water low	Source strength No. 3.

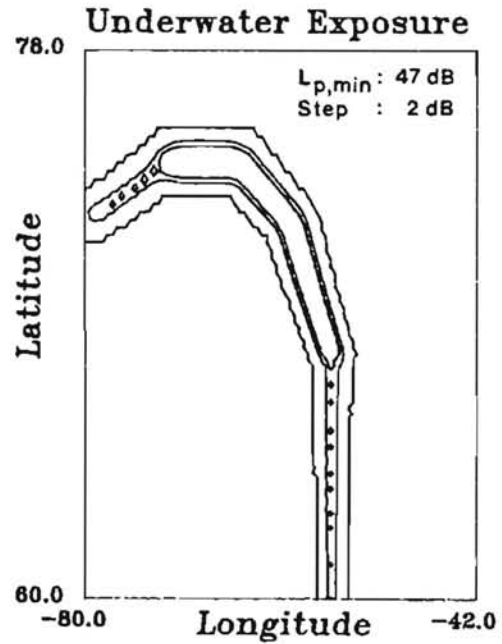
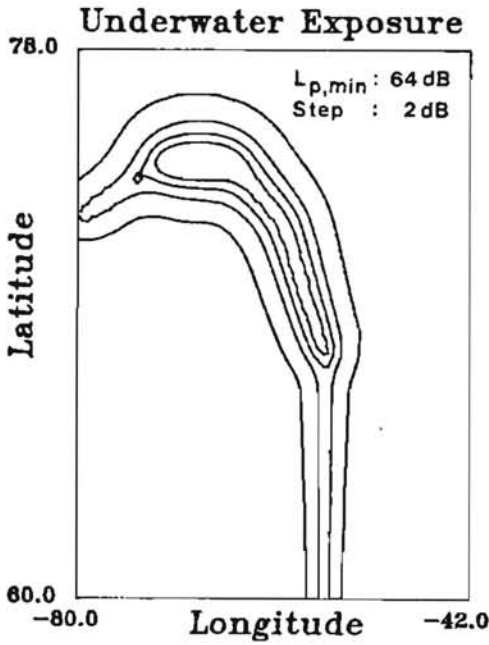
The ambient noise is the "Arctic Winter" given as background noise No. 2 in Table 6.3.

The results are given in figure 6.5. The varying source strength conditions are clearly seen in the results from example 3. The contour lines spread out at route points 3 and 4 due to the increase in source strength at these points.



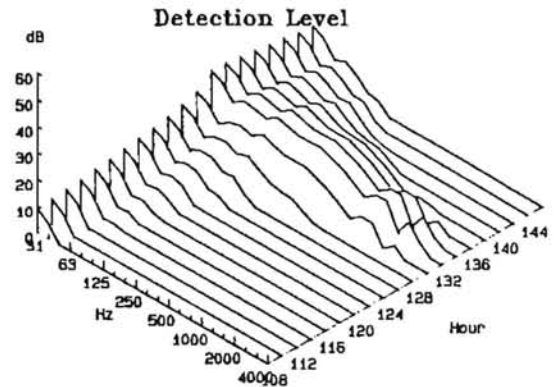
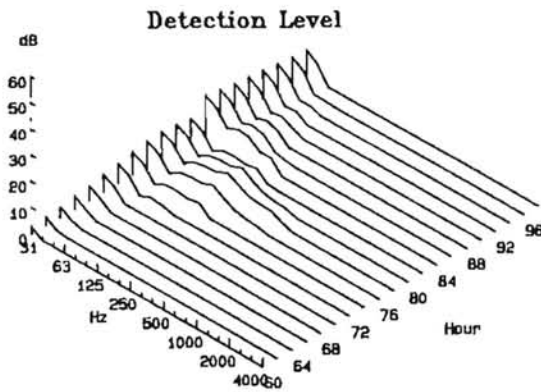
100 HZ:

1000 HZ:



Disko (69°N, 54°W):

Kap York (76°N, 66°W):



Input:

```

=====
ROUTE: 9  POSITION NO.    LAT.    LONG.    BACK.  PROFILE TIME
=====
-1  MAIN DATA  76: 0: 0  -66: 0: 0    2      1    2.0
=====
POSITION NO.(1-20)  LAT.    LONG.    SOURCE  DEPTH  SEA
=====
1      56: 0: 0  -56: 0: 0    1     1000   0
2      60: 0: 0  -56: 0: 0    1      500   0
3      70: 0: 0  -56: 0: 0    2      300   0
4      74: 0: 0  -60: 0: 0    2      500   0
5      75:30: 0  -65: 0: 0    4      400   0
6      75:30: 0  -72: 0: 0    1      400   0
7      74: 0: 0  -80: 0: 0    3      500   0
8      74: 0: 0  -85: 0: 0    3      500   0
11     0: 0: 0    0: 0: 0    0         0   0
=====

```

Figure 6.5.
Example 3. Icebreaker sailing along West Greenland route during winter conditions.



The passage of the observation point at Disko is seen to occur approximately 80 hours after the start. The increase in source strength at route point 3 can be seen when reaching 84 hours. A strong influence at the Kap York observation point can be seen in the detection level. In this case the route passes rather close by the observation point and consequently the detection level is high even at high frequencies. The variations in the detection level spectra are due to the variations in the transmission loss with frequency. It can be seen that even at 2000 Hz the ambient noise is exceeded for approximately 12 hours at the observation point during a passage of the ship. Also it can be seen how the high frequency parts of the spectra are attenuated more than the low frequency parts due to the transmission.

Example 4

In this example the expected source strength of a LNG-carrier, as planned for the Arctic Pilot Project, has been assumed for a ship sailing along the central route during winter conditions.

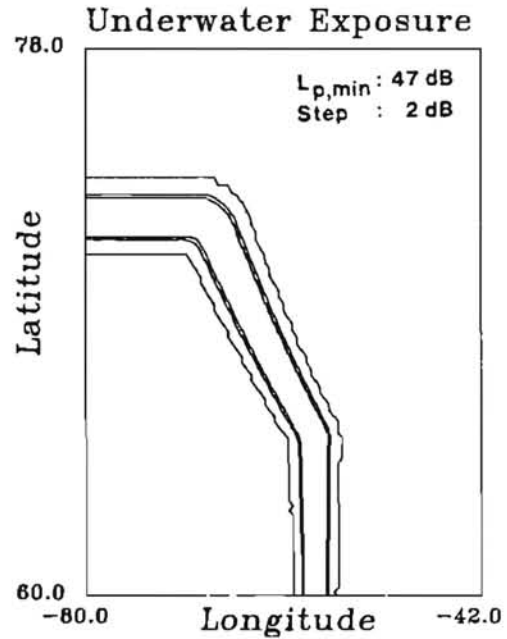
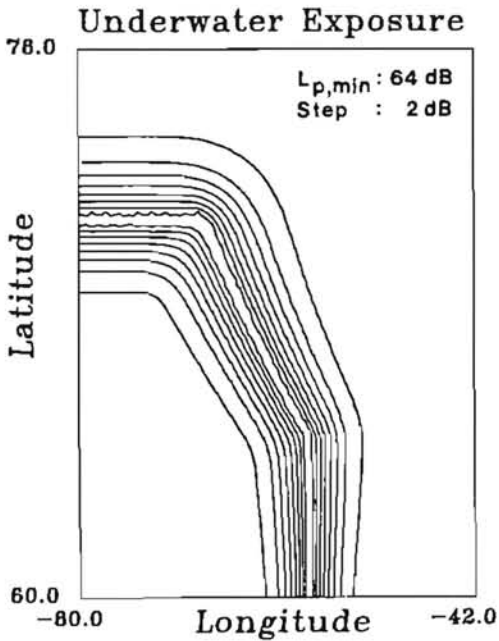
The source strength applied has been found from the levels suggested by N. Brown in reference /28/. The condition, full power in ice, 12 knots, has been selected. The source strength has been modified with a lower peak frequency as described in Section 2.1. The source strength is kept constant during the entire route and the magnitude can be found for source strength No. 5 in Table 6.1.

The results are presented in Figure 6.6. It can be noted that the extent of exposure is larger than in example 2 due to the higher source strength of the APP tanker compared with the icebreaker. The high source strength, especially at low frequencies can be seen in the detection levels where the low frequency part is very pronounced.



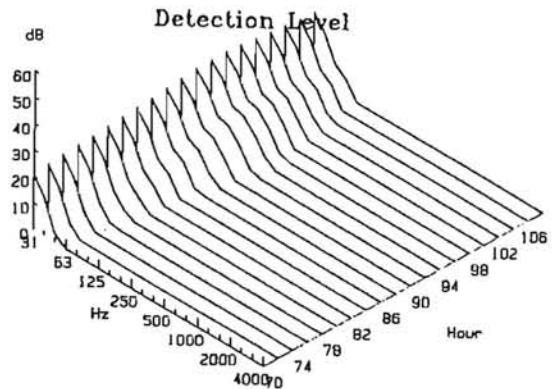
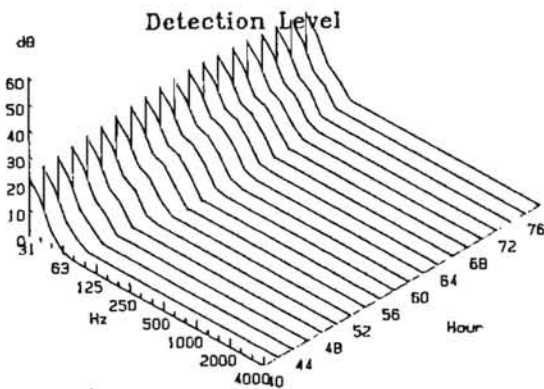
100 HZ:

1000 HZ:



Disko (69°N, 54°W):

Kap York (76°N, 66°W):



Input:

```

=====
ROUTE: 5  POSITION NO.      LAT.    LONG.    BACK.  PROFILE TIME
=====
-1  MAIN DATA  76: 0: 0  -66: 0: 0    2      1    2.0
=====
POSITION NO.(1-20)  LAT.    LONG.    SOURCE  DEPTH  SEA
-----
1                   56: 0: 0  -58: 0: 0    5     2000   1
2                   60: 0: 0  -58: 0: 0    5     3000   1
3                   67: 0: 0  -58: 0: 0    5      800   1
4                   74: 0: 0  -68: 0: 0    5     2000   1
5                   74: 0: 0  -80: 0: 0    5      800   1
6                   74: 0: 0  -85: 0: 0    5      800   1

```

Figure 6.6.

Example 4. LNG-carrier sailing along the central route during winter conditions.



Example 5

This last example illustrates the passage of a ship which is not an icebreaker. The source strength of a seismic ship of typical size is calculated and used for the example as shipping of this kind is likely to occur in the area. The magnitude of the source strength is calculated by the prediction model described in Section 2.1 assuming the following propeller data:

Diameter : 2.2 m
Revolutional speed: 150 RPM
No. of blades : 4
Area of cavitation: $A_C/A_D = 0.1$
Peak frequency : 100 Hz

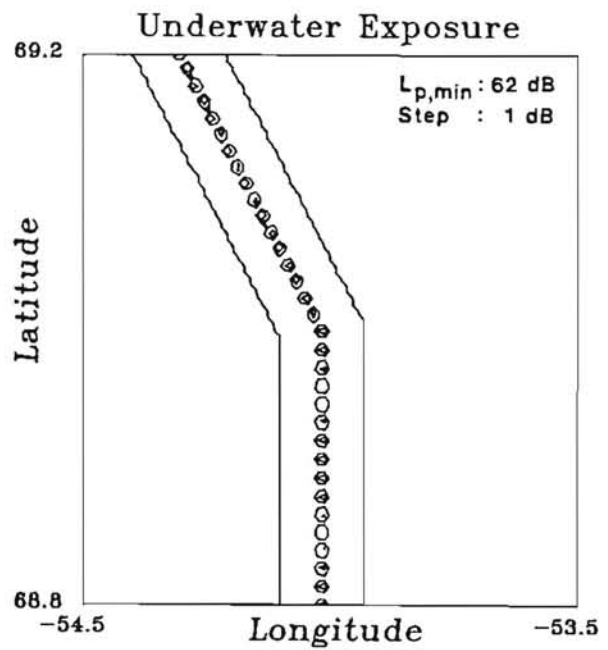
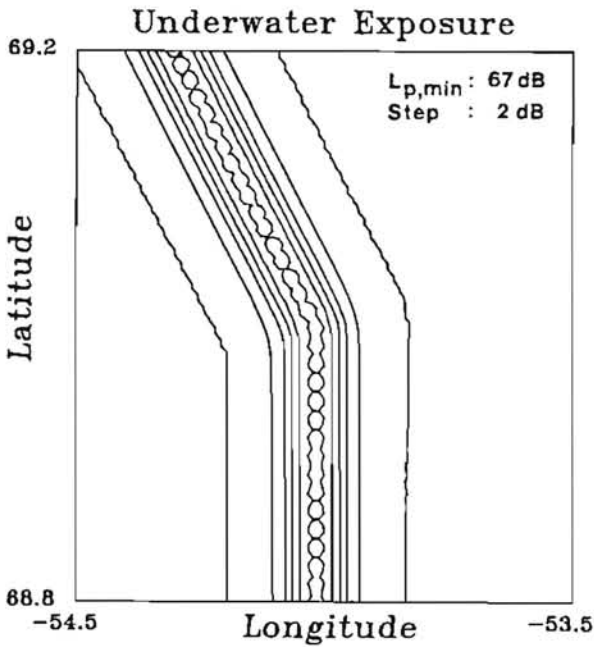
The source strength of the seismic ship (No. 7 in Table 6.1) is much lower than for the icebreaker. The speed normally applied during seismic work is as low as 4 knots. The combination of low speed and low source strength results in very low equivalent (time averaged) noise levels along the long routes applied for the first three examples. The exposure therefore has been calculated for a short route in this last example. The area used for the exposure map is approximately 60 x 40 nautical miles covering most of the short route defined by 3 points.

The results are given in Figure 6.7. The contour plots are again parallel to the route as the source strength is constant along the route. At 100 Hz the distance from the route to the last contour line is approximately 4 Nm. This means that the equivalent noise level at 100 Hz, averaged over the time used by the ship to pass the route, is equal to the ambient noise level at a distance of 4Nm from the route. At 100 Hz this distance is reduce to approximately 1.8 Nm.

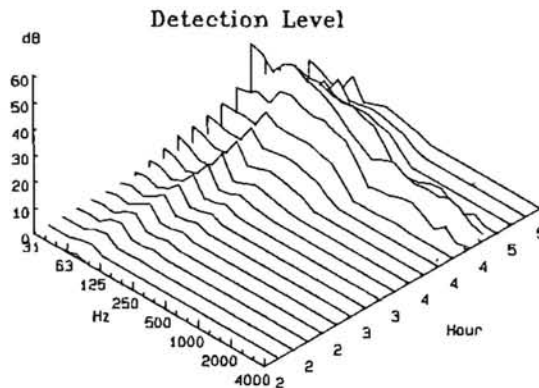


100 HZ:

1000 HZ:



Disko (69°N, 54°W):



Input:

```

=====
ROUTE: 6 POSITION NO.    LAT.    LONG.    BACK.    PROFILE TIME
=====
-1  MAIN DATA  69: 0: 0  -54: 0: 0    1      0      .2
=====
POSITION NO.(1-20)  LAT.    LONG.    SOURCE  DEPTH  SEA
-----
1                   68:40: 0  -54: 1: 0    6      500   0
2                   69: 0: 0  -54: 1: 0    6      500   0
3                   69:20: 0  -54:30: 0    6      500   0

```

Figure 6.7.

Example 5. Seismic ship passing Disko Island during summer conditions. It should be noted that the area used in this example is much smaller than in the other examples.



6.3 Discussion

The previous examples illustrate the use of the exposure programme and the type of results to be obtained. It is important to note that the accuracy of the results obtained by using this programme of course depend on the accuracy of the input data applied and the assumptions made for the programme.

The input data, which are the source strength, transmission loss and ambient noise, have to be simplified to a great extent compared with the real conditions. Especially, the transmission loss is connected with a rather high uncertainty due to the very complex nature of sound propagation in the sea. Consequently, it is preferable to use the exposure programme with measured transmission loss data from the area which is actually being investigated. Unfortunately, this is often impossible and the transmission loss should therefore be calculated separately by a prediction model with a high degree of accuracy.

The prediction model presently incorporated in the programme is only intended to be used if no other data are available. In this model, the effect of the ice-cover is very strong and must be regarded as a "maximum loss" case. The additional loss caused by the ice-cover is mainly due to the rough underside of the ice which gives rise to scattering of the sound waves. If a lower effect of the ice-cover is wanted, it is possible to use the model with the open water condition and account for the ice-cover by selecting the magnitude of the sea state. It can be noted that the transmission loss is calculated by the programme to be of the same magnitude in the ice-covered condition as for the open water condition with sea state 10.

The main simplification performed during the development of the exposure programme is also connected with the transmission loss. It is assumed that the transmission loss is constant in all directions. This assumption makes it impossible to model e.g. a route close to a coast line where the transmission loss is bound



to differ with regard to the direction of the coast compared with the direction into the open sea. This problem is illustrated clearly in the examples where the contour lines often exceed the coast line of Greenland or Lancaster Sound. However, the possibility of using different transmission losses in different directions would complicate the programme to an extent exceeding the aim of this work. If a route is located close to a coast it is suggested to divide the calculations into two parts with two different sets of sound transmission loss data.



REFERENCES

1. Urick, R.J.: "Principles of Underwater Sound" 2nd ed. McGraw Hill Book Company 1975.
2. Ross, D.: "Mechanics of Underwater Noise". Pergamon Press, 1976.
3. Baiter, H.-J.; Gruneis, F. and Tilmann, P.: "An Extended Base for the Statistical Description of Cavitation Noise". International Symposium on Cavitation Noise, ASME, Winter Annual Meeting, 1982.
4. Brown, N.: "Cavitation Noise Problems and Solutions". Proceedings from International Symposium on Shipboard Acoustics. Delft 1976.
5. Brown, N.: "Revisions to the the Integrated Route Analysis", Volume 2, Section 3.2.3.1 (Source Level Estimates). The Arctic Pilot Project, Calgary, April 1981.
6. Thiele, L.: "Underwater Noise from the Icebreaker M/S VOIMA". Report 81.42, Ødegaard & Danneskiold-Samsøe ApS, 1981.
7. Marsh, H.W., Schulkin, M.: "Shallow Water Transmission". Journal of Acoustical Society of America, 34, 1962, pp. 863-864.
8. Thiele, L.: "Underwater Noise from the Propellers of a Triple Screw Containership". Report 82.54, Ødegaard & Danneskiold-Samsøe ApS, 1982.
9. Thiele, L.: "Underwater Noise Study from the Icebreaker John A. MacDonald". Report 85.133, Ødegaard & Danneskiold-Samsøe ApS, 1988.



10. Leggat, L.J.: "Analysis of the Underwater Noise of CCGS John A. MacDonald". Technical memorandum 85/223, Defence Research Establishment Atlantic, 1985.
11. Greene, C.R.: "Underice Radiated Noise Measurements of the Icebreaker CCGS John A. MacDonald in Baffin Bay and Lancaster Sound, June 1983". Greenridge Sciences, Inc., 1984.
12. Mellen, Browning and Ross: "Attenuation in Randomly Inhomogeneous Sound Channels". Journal of the Acoustical Society of America, Vol. 56, No. 1, 1974, pp. 80-82.
13. Thorp: "Deep-Ocean Sound Attenuation in the Sub- and Low-Kilocycle-per-Second Region". Journal of the Acoustical Society of America, Vol. 38, 1965, pp. 648-654.
14. Urick, R.J.: "Ambient Noise in the Sea". Peninsula Publishing 1986.
15. Milne, A.R. and Ganton, J.H.: "Ambient Noise under Arctic Sea Ice". Journal of the Acoustical Society of America, Vol. 36, No. 5, 1964, pp. 855-863.
16. Knudsen, V.O.; Alford, R.S. and Emling, J.W.: "Underwater Ambient Noise". Journal of Marine Research. Vol. 7, pp. 410, 1948.
17. Diachok, O.I. and Winokur, R.S.: " Spatial Variability of Underwater Ambient Noise at the Arctic Ice-Water Boundary". Journal of the Acoustical Society of America. Vol. 55, No. 4, 1974, pp. 750-753.
18. Leggat, L.J.; Merklinger, H.M. and Kennedy, J.L.: "LNG-Carrier. Underwater Noise Study for Baffin Bay. The Question of Sound from Icebreaker Operations". Proceedings of a Workshop. Toronto 1981. Petro Canada, Calgary, Alberta.



19. Thiele, L.: "Noise in the Sea off Scoresbysund, East Greenland". Report 82.45, Ødegaard & Danneskiold-Samsøe ApS, 1982.
20. Thiele, L.: "Ambient Noise in the Sea off Kap York, Melville Bay, North West Greenland". Report 82.53, Ødegaard & Danneskiold-Samsøe ApS, 1982.
21. Thiele, L.: "Ambient Noise in the Sea off Thule, North Greenland". Report 83.88, Ødegaard & Danneskiold-Samsøe ApS, 1983.
22. Clay, C.S. and Medwin, H.: "Acoustical Oceanography". Wiley-Interscience, 1977.
23. Tolstoy, I. and Clay, C.S.: "Ocean Acoustics. Theory and Experiment in Underwater Sound". The Acoustical Society of America, 1987.
24. Rasmussen, K.B. and Vistisen, B.: "Calculation of Underwater Sound Propagation by Means of a FFP Model". Report 86.149, Ødegaard & Danneskiold-Samsøe ApS, 1986 (In Danish).
25. Vilmann, O., Gerstoft, P. and Krenk, S.: "High-Speed Forward Modelling in Seismic Data Processing". Final report 1 and 2, EEC Contract EN3C-0010-DK(MB), 1989.
26. Diachok, O.I.: "Effects of Sea-Ice Ridges on Sound Propagation in the Arctic Ocean". Journal of the Acoustical Society of America. Vol. 59, No. 5, pp. 1110-1120, 1976.
27. Baker, W.F.: "New Formula for Calculating Acoustic Propagation Loss in a Surface Duct in the Sea". Journal of the Acoustical Society of America. Vol. 57, No. 5, pp. 1198-1200, 1975.
28. Brown, N.: "Revisions to the Integrated Route Analysis", Volume 2, Section 3.2.3.1, Arctic Pilot Project, Calgary, April 1981.

Ødegaard & Danneskiold-Samsøe ApS

Rådgivende ingeniører - Støj og vibrationer
Consulting Engineers - Noise and Vibration

Krogsgade 1
DK-2100 Copenhagen Ø
Denmark
Telephone: 01 26 60 11
Telex: 19710 oedan dk
Telefax: 01 26 50 18

